

Bridging Control with Neural Network Verifier α - β -CROWN: A Tutorial

Haoyu Li*, Xiangru Zhong*, Hao Cheng, Bin Hu, Huan Zhang

Abstract—Learning-based methods for synthesizing controllers have gained popularity due to their high expressiveness and strong empirical performance. However, in safety-critical scenarios such as autonomous driving, robotics, and power systems, empirical performance alone is insufficient, and formal verification of controller properties such as stability and safety is highly desirable. Unfortunately, many prior verification approaches are either tied to specific structural assumptions on the system or the certificate, making them difficult to transfer across settings, or suffer from poor scalability on higher-dimensional neural network systems. In this tutorial, we present a unified framework that aims to mitigate this gap via bridging control with the state-of-the-art neural network verifier α , β -CROWN (alpha-beta-CROWN). At its core, α , β -CROWN is a general-purpose bounding engine for nonlinear functions represented as computation graphs: given an input domain, it can automatically produce certified bounds and explicit linear relaxation of the nonlinear function. These certified bounds are useful on their own for tasks such as reachability analysis and local linear approximation, and they also provide the foundation for more complex routines that perform verification, satisfiability checking, and optimization. More specifically, many control problems reduce to verifying real-valued inequalities over a state domain (e.g., Lyapunov theory and barrier functions). Consequently, α , β -CROWN enables scalable verification of such conditions by computing tight bounds on these conditions and recursively partitioning and pruning subdomains based on the bounds. Thanks to GPU parallelization, this pipeline demonstrates superior scalability on verification and optimization problems that are challenging for traditional approaches. In this tutorial, we discuss the basics of α , β -CROWN, and introduce its application to various control-related tasks. Finally, we will discuss training frameworks for co-synthesizing controllers and corresponding verifier-friendly certificates.

I. INTRODUCTION

Learning-based neural network (NN) control policies have become increasingly prevalent in modern control applications, including autonomous vehicles, robotic manipulations, and power system regulations [1]–[3]. Their expressive capacity enables the synthesis of control policies for general nonlinear plants [4]. However, the deployment of such controllers in safety-critical settings requires guarantees that cannot be obtained through empirical testing alone. As a matter of fact, there is a growing demand for formal verification frameworks capable of certifying closed-loop properties such as stability and safety for learned NN controllers [5], [6].

* Equal Contribution

Haoyu Li is with the Department of Computer Science, and Xiangru Zhong, Hao Cheng, Bin Hu, Huan Zhang are with the Department of Electrical and Computer Engineering, University of Illinois Urbana-Champaign, Urbana, IL 61801, USA haoyuli5@illinois.edu, xiangru4@illinois.edu, haoc539@illinois.edu, binhu7@illinois.edu, huan@huan-zhang.com

A natural formulation is to cast verification of NN controllers as a nonlinear satisfiability problem and solve it with a general-purpose SMT verifier or other nonlinear programming solvers. In this vein, existing works formulate the closed-loop verification objective as a constraint system and invoke SMT solvers [7]–[15] (e.g., dReal [16] and Z3 [17]), MILP/MIP-based encodings for piecewise-linear (ReLU/LeakyReLU activations) networks [18]–[23], or convex optimization problems such as semidefinite programming (SDP) or sum-of-squares (SOS) programming [24]–[33]. However, these methods typically scale poorly due to the limited ability to exploit GPU-acceleration and parallelism. In addition, methods such as SOS/MILP can only handle problems with specific structures, for example, relatively shallow piecewise-linear networks with ReLU-type activations, or polynomials [18]–[20]. Recent control-oriented verification methods also exploit certificate-specific structure, for example, through symbolic bound propagation [34]–[38]. While effective for their target properties, these pipelines are less directly transferable across different certificate classes.

In the machine learning community, NN verification has emerged as an important direction for scalable certification [39]–[46]. Rather than solving the nonlinear constraints exactly as done in SMT or MILP-based approaches, one can construct sound over-approximations of the network’s behavior over a given input set [44], [47]. Built upon this idea, α , β -CROWN has become a state-of-the-art NN verifier that combines linear bound propagation with branch-and-bound [44], [48]–[56] to achieve several key advantages. First, α , β -CROWN directly works on general nonlinear functions represented by computation graphs, enabling the direct handling of constraints and objectives with complex NN components [57]–[61]. Secondly, α , β -CROWN exhibits much stronger empirical scalability. Notice that α , β -CROWN propagates sound and efficient linear over-approximations of the computation graph in a very efficient manner, and uses branch-and-bound to iteratively partition and tighten those subdomains whose bounds remain inconclusive. The efficient bound propagation in α , β -CROWN is accelerated by GPUs, and a large number of subdomains can be calculated in parallel, which makes the verification process very efficient. Finally, the linear bound propagation algorithm in α , β -CROWN is fully differentiable, enabling more downstream applications such as training verification-friendly controllers [58].

The properties of α , β -CROWN enable several use modes for control problems. First, the verifier could return certified numeric bounds as well as local linear bounds of a

complicated nonlinear function represented as a computation graph. These bounds can be directly used for reachability analysis [62]–[68] and for constructing local linear approximations of nonlinear functions [69]–[73]. Second, the same bounds can be used for solving general satisfiability problems over real arithmetic. This enables scalable certification of many control theoretic properties, such as Lyapunov stability [74]–[76], Barrier function safety [77]–[80], or contraction [81]–[84]. Finally, the verifier can be used as an optimizer for general nonlinear objectives, such as MPC style optimization with general nonlinear models [85]. Building on these capabilities, this tutorial shows how to reformulate common control-theoretic problems amenable to α, β -CROWN. Additionally, we illustrate how to jointly synthesize verifiable controllers together with neural certificates with counterexample-guided Synthesis (CEGIS) [7], [14], [57], [86]–[91] or certified training [39], [58], [92]. In summary, the goals of this tutorial are:

- Provide the mathematical background of the neural network verifier α, β -CROWN.
- Demonstrate how to formulate control problems, such as reachability, satisfiability (Lyapunov and Barrier function verification), and optimization (MPC), in an α, β -CROWN-friendly manner.
- Detail the programming interface and practical usage of α, β -CROWN.
- Introduce several training paradigms that can yield verifiable neural certificates.

II. MOTIVATING EXAMPLES

To make the capabilities of α, β -CROWN concrete, in this section, we illustrate each mode of α, β -CROWN with simple motivating examples. More detailed applications to control will be deferred to Section V and IV. All the examples provided in this section will consider a discrete-time system

$$x_{t+1} = f(x_t, u_t) \quad (1)$$

where $x_t \in \mathbb{R}^n$ is the state, $u_t \in \mathbb{R}^m$ is the control input, and f may be a general nonlinear dynamics model (including learned neural dynamics). When a state-feedback controller $u_t = \pi(x_t)$ is applied, the resulting closed-loop system is

$$x_{t+1} = f(x_t, \pi(x_t)) =: g(x_t), \quad (2)$$

where g denotes the induced closed-loop map.¹

A. α, β -CROWN for Computing Certified Bounds

We first illustrate a simple use case of the bounds α, β -CROWN produced. Given an input domain \mathcal{B} for which the initial state belongs, it is oftentimes of interest to compute an overapproximation of the one-step reachable set, i.e., the set of all possible $x_1 = g(x_0)$ for $x_0 \in \mathcal{B}$. Even this one-step problem is nontrivial when g contains NN components. In this scenario, α, β -CROWN serves to compute certified bounds of the function g over \mathcal{B} , yielding a sound enclosure:

¹The complete code for all examples in this tutorial is available at https://github.com/Verified-Intelligence/abCROWN-Control_Tutorial.

Compute Bounds in α, β -CROWN

$$\text{Find } \underline{x}, \bar{x} \in \mathbb{R}^n \text{ such that } g(\mathcal{B}) \subseteq [\underline{x}, \bar{x}], \quad (3)$$

where $[\underline{x}, \bar{x}] = \{x \in \mathbb{R}^n : \underline{x} \leq x \leq \bar{x}\}$ denotes an elementwise-box. Unrolling this process step by step allows scalable reachability analysis over very general function classes, including learning-based dynamics with neural networks.

```

1 from abcrown import (
2     ABCrownSolver,
3     ConfigBuilder,
4     IOConstraints,
5     input_vars,
6     output_vars,
7 )
8 # Note: These imports are needed for all the
9 # following examples.
10 # 1. Define and instantiate the computation
11 # graph
12 class ReachabilityGraph(nn.Module):
13     def __init__(self):
14         super().__init__()
15         self.dt = 0.1
16         # A residual neural network dynamics
17         model: x_{t+1} = x_t + dt * NN(x_t)
18         self.net = nn.Sequential(
19             nn.Linear(1, 16),
20             nn.ReLU(),
21             nn.Linear(16, 16),
22             nn.ReLU(),
23             nn.Linear(16, 1)
24         )
25     def forward(self, x_t):
26         # The computation graph natively
27         # supports standard PyTorch arithmetic
28         return x_t + self.dt * self.net(x_t)
29
30 computation_graph = ReachabilityGraph()
31 # 2. Define graph input and output variables
32 x = input_vars(1)
33 y = output_vars(1)
34 # 3. Create solver instance with the
35 # computation graph
36 cfg = ConfigBuilder.from_defaults().set(
37     "bab/timeout", 30)
38 solver = ABCrownSolver(computation_graph, x, y,
39     config=cfg)
40 # 4. Create input constraints
41 # Bounding the initial state within a domain D
42 input_constraints = (x >= -1.0) & (x <= 1.0)
43 constraints = IOConstraints(
44     input_vars=x,
45     input_constraints=input_constraints
46 )
47 # 5. Compute bounds on y given constraints on x
48 result = solver.compute_bounds(
49     constraints=constraints,
50     objective=y
51 )
52
53 print("Lower bounds: ", result.lower)
54 print("Upper bounds: ", result.upper)

```

B. α, β -CROWN for Solving Satisfiability Problems

We then consider an example of using α, β -CROWN for solving a satisfiability problem. Formally certifying properties of neural network-controlled dynamical systems, such as stability or safety guarantees, is non-trivial. For example, the standard strategy to prove the stability of (1) is through Lyapunov functions [93], [94]. Formally, suppose there is a domain \mathcal{B} around the equilibrium x^* such that there exists a function $V : \mathcal{B} \rightarrow \mathbb{R}$ such that

- 1) $V(x^*) = 0$ and $V(x) > 0$ otherwise,
- 2) $V(g(x)) < V(x)$ for all $x \neq x^*$,

then x^* is asymptotically stable. Suppose that we have a candidate V that satisfies $V(x^*) = 0$ and $V(x) > 0$ otherwise (e.g., by construction [57]), α, β -CROWN enables efficient verification of the following satisfiability problem:

Verifying Satisfiability Problems in α, β -CROWN

$$V(f(x, \pi(x))) - V(x) < \varepsilon \quad \forall x \in \mathcal{B}.$$

where $\varepsilon > 0$ is a small tolerance used to handle the equilibrium. Here, the condition is simplified. In Section IV-B, we provide a more detailed discussion on ROA verification in α, β -CROWN. As a high-level intuition, α, β -CROWN converts the condition into a bound computation problem and compares the resulting bounds with 0. Users define the verification specification using a Python-embedded DSL (Domain-Specific Language), and call α, β -CROWN to verify it.

```

1 # 1. Define a control system and a Lyapunov
  function
2 dynamics = get_dynamics_model()      # f(x, u)
3 controller = get_controller()        # pi(x)
4 lyapunov = get_lyapunov_network()    # V(x)
5
6 # 2. Build the computation graph
7 # We assume this graph outputs a vector y:
8 # y[0] = V(f(x, pi(x))) - V(x) + kappa * V(x)
9 model = DiscreteLyapunovGraph(
10     dynamics, controller, lyapunov, kappa=0.1)
11
12 # 3. Define graph input and output variables
13 x = input_vars(2)                    # Input dimension is 2
14 y = output_vars(1)                   # Output dimension is 1
15
16 # 4. Create solver instance with the graph
17 solver = ABCrownSolver(model, x, y)
18
19 # 5. Create verification constraints.
20 input_constraints = (
21     (x >= [-2.0, -2.0]) &
22     (x <= [2.0, 2.0])
23 )
24 output_constraints = (
25     (y[0] < 1e-6)
26 )
27
28 constraints = IOConstraints(
29     input_vars=x,
30     output_vars=y,
31     input_constraints=input_constraints,
32     output_constraints=output_constraints,
33 )
34

```

```

35 # 6. Run verification.
36 result = solver.verify(constraints=constraints)
37
38 print("Status:", result.status)
39 # "verified", "falsified", "unknown".

```

Although simple, this problem is a good general template for satisfiability problems: many control specifications reduce to verifying the sign of a scalar expression over a domain \mathcal{B} . In α, β -CROWN, switching from Lyapunov to other properties usually amounts to changing only a few lines of PyTorch code, while the whole verification pipeline remains the same. While here we used a discrete-time system as an example, α, β -CROWN can also handle continuous-time systems with Jacobians.

C. α, β -CROWN for Non-linear Optimization

Finally, we illustrate the use of α, β -CROWN as an optimizer with an example of a finite horizon MPC problem. A common goal for planning problems in control is to find a sequence of optimal actions u_t such that the sum of the step cost is minimized, i.e.

MPC optimization in α, β -CROWN

$$\min_{u_t \in \mathcal{U}} \sum_{t=t_0}^{t_0+H} c(x_t, u_t), \quad \text{s.t. } x_{t+1} = f(x_t, u_t) \quad (4)$$

with c being the cost function. Since in many cases f will be a learning-based dynamics, the optimization problem is highly non-convex and nonlinear, especially when the horizon is long. The key observation is that, although complicated, the total cost function $\sum_{t=t_0}^{t_0+H} c(x_t, u_t)$ can be treated as a computation graph that maps \mathcal{U}^H to \mathbb{R} . Therefore, α, β -CROWN can efficiently and systematically handle this optimization problem. Compared to directly applying gradient descent, which is fast but typically provides only a local minimum, α, β -CROWN is theoretically a global optimizer guided by certified lower bounds, which can be used as a signal for optimality gap. More details of the optimizer functionality are discussed in Section VII-A.

```

1 # 1. Load the model
2 model = get_MPCGraph(horizon=H)
3
4 # 2. Define graph input and output variables
5 u = input_vars(H)
6 y = output_vars(1)
7
8 # 3. Build the solver
9 solver = ABCrownSolver(model, u, y)
10
11 # 4. Create constraints
12 input_constraints = (u >= -5.0) & (u <= 5.0)
13 constraints = IOConstraints(
14     input_vars=u,
15     input_constraints=input_constraints,
16 )
17
18 # 5. Minimize the total cost
19 result = solver.minimize(
20     objective=y[0],

```

```

21 constraints=constraints)
22
23 print(f"Minimum cost found: {
24     result.primal_value}")
25 print(f"Optimal action sequence: {
26     result.x_best}")

```

III. THE α, β -CROWN VERIFIER

Formally, α, β -CROWN aims to verify

$$F(x) > 0 \text{ for all } x \in \mathcal{B} \quad (5)$$

with F composed by supported nonlinear functions and \mathcal{B} being a hyper-rectangle with the same dimension as x . α, β -CROWN couples fast *symbolic linear bound propagation* with *branch-and-bound*. For a hyper-rectangle \mathcal{B} , it constructs an affine lower bound of F and provides certification based on the minimum value of this affine bound. If inconclusive, it *splits* \mathcal{B} into sub-domains and repeats. As the domains shrink, local linear relaxations tighten, and the overapproximation error from the nonlinearities decreases. The full process is highly efficient, as all necessary computations, including local relaxations and bound propagations, are heavily vectorized and can be executed in parallel. Tens of thousands of sub-domains can be processed simultaneously on a GPU, enabling rapid pruning of large regions and certification with only coarse bounds on tiny domains.

A. Admissible Function Class

In control applications, as seen in Section II, the objective we wish to verify is rarely just a standalone neural network. More often, it is an expression that comprises several pieces: a policy $\pi(x)$, system dynamics $f(x, u)$, and some neural certificates $V(x)$. However, all these functions belong to a more generic function class named **computation graphs**. Intuitively, a computation graph is a directed acyclic graph (DAG) that represents a complicated function as a sequence of simple steps. Each node in the computation graph is an elementary operation (like addition, multiplication, or ReLU), and each edge passes the results of one step to the next. More formally, a computation graph can be defined as follows.

Definition 1 (Computation Graph): A computation graph is a finite directed acyclic graph (DAG) $G = (V, E)$ whose nodes $V = \{1, \dots, n\}$ are partitioned into input nodes V_{in} , parameter/constant nodes V_{par} , and operator nodes V_{op} . Each node i has an associated output vector $h_i \in \mathbb{R}^{d_i}$. For each node i , let $u(i) = (u_1(i), \dots, u_{m(i)}(i))$ be the ordered list of its parents (so $(u_j(i), i) \in E$ and $m(i) = |u(i)|$).

Inputs. For every input node $i \in V_{\text{in}}$ we associate an external input variable $x_i \in \mathbb{R}^{d_i}$, and the node simply passes it through: $h_i = x_i$. If admissible sets $S_i \subseteq \mathbb{R}^{d_i}$ are specified for the inputs, the input space is $S := \prod_{i \in V_{\text{in}}} S_i$, and we write $x = (x_i)_{i \in V_{\text{in}}} \in S$.

Parameters. For every parameter/constant node $i \in V_{\text{par}}$ a fixed vector $c_i \in \mathbb{R}^{d_i}$ is given, and $h_i = c_i$.

Operators. For every operator node $i \in V_{\text{op}}$ a primitive map

$$H_i : \prod_{k=1}^{m(i)} \mathbb{R}^{d_{u_k(i)}} \longrightarrow \mathbb{R}^{d_i}$$

is specified (affine map, elementwise nonlinearity, concatenation, reduction, etc.), and its output is

$$h_i = H_i(h_{u_1(i)}, \dots, h_{u_{m(i)}(i)}).$$

Outputs. Let $O \subseteq V$ denote the set of output nodes (i.e., nodes with an out-degree of 0). The graph then induces the function

$$F_G : \prod_{i \in V_{\text{in}}} \mathbb{R}^{d_i} \longrightarrow \prod_{o \in O} \mathbb{R}^{d_o}, \quad F_G(x) = (h_o)_{o \in O}.$$

Example 1 (Toy Computation Graph): Suppose we want to represent the function

$$f(x) = \text{ReLU}(2x - 1) + 3. \quad (6)$$

This can be written as a computation graph with four operator nodes: (1) multiply input by 2, (2) subtract 1, (3) apply ReLU, then (4) add 3. Each intermediate value is stored at a node, and the edges show how values flow from one step to the next. As shown in Figure 1, this small example illustrates the general idea: even a simple function can be broken down into basic operations, which is exactly how α, β -CROWN reasons about much larger networks.

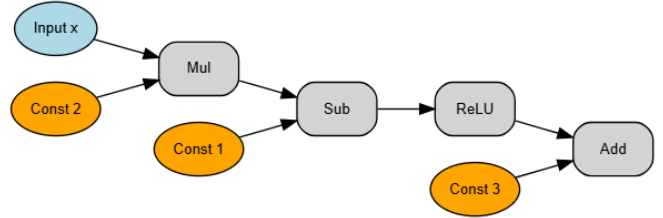


Fig. 1. Computation graph of Equation (6).

The abstraction above captures many models and specifications that are commonly used in learning and control. For example, it is clear that any standard feed-forward network or more complicated neural network structures, such as residual networks or transformers, can be specified in this form with an appropriate choice of nodes, edges, and operators. Furthermore, many interesting properties of control systems, such as the Lyapunov condition, can be specified in this form. For example, for a discrete time system $x_{t+1} = f(x_t, \pi(x_t))$, the Lyapunov condition

$$F(x) = V(x) - V(f(x, \pi(x))) \quad (7)$$

is also a computation graph even when $\pi(x)$ and $V(x)$ are parametrized by neural networks (See Figure 2).

B. auto-LirPA: Automatic Linear Relaxation based Perturbation Analysis

Suppose $F : \mathbb{R}^n \rightarrow \mathbb{R}$ is a computation graph (e.g., Fig. 2) and verification domain is an L_∞ box $\mathcal{B} = \prod_{i=1}^n [\ell_i, u_i]$. α, β -CROWN efficiently verifies condition (5) by propagating

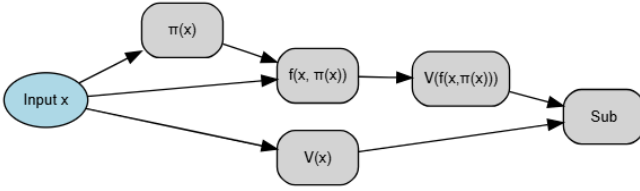


Fig. 2. Computation graph of the Lyapunov condition. For illustration, f , π , and V are abstracted as single nodes.

symbolic bounds on F over domain \mathcal{B} to get the linear lower bound of F on \mathcal{B} , i.e., compute $\underline{a} \in \mathbb{R}^n, \underline{b} \in \mathbb{R}$ with

$$F(x) \geq \underline{a}^\top x + \underline{b}, \quad \forall x \in \mathcal{B} \quad (8)$$

We then claim verification successful if

$$\inf_{x \in \mathcal{B}} \underline{a}^\top x + \underline{b} = (\underline{a}^+)^T \ell + (\underline{a}^-)^T u + \underline{b} > 0 \quad (9)$$

holds with $\underline{a}^+ = \max(\underline{a}, 0)$ and $\underline{a}^- = \min(\underline{a}, 0)$. To enable symbolic linear bound propagation with the full computation graph, we need to perform a **linear relaxation** of all primitive operators H_i , defined as follows.

Definition 2 (Linear relaxation): Let $h : \prod_{j=1}^n \mathbb{R}^{p_j} \rightarrow \mathbb{R}^q$ and let the input domain be a product box $Z = \prod_{j=1}^n [\ell_j, u_j]$, with $\ell_j, u_j \in \mathbb{R}^{p_j}$. A *linear relaxation* of h on Z is any collection of matrices and vectors

$$\{A_\ell^{(j)}, A_u^{(j)} \in \mathbb{R}^{q \times p_j}\}_{j=1}^n, \quad b_\ell, b_u \in \mathbb{R}^q$$

such that for all $(x_1, \dots, x_n) \in Z$ the elementwise inequalities hold:

$$\sum_{j=1}^n A_\ell^{(j)} x_j + b_\ell \leq h(x_1, \dots, x_n) \leq \sum_{j=1}^n A_u^{(j)} x_j + b_u.$$

Equivalently, stacking $x = \text{col}(x_1, \dots, x_n) \in \mathbb{R}^p$ with $p = \sum_j p_j$ and similarly defining the global bounds $\ell = \text{col}(\ell_1, \dots, \ell_n)$ and $u = \text{col}(u_1, \dots, u_n)$ such that $Z = [\ell, u]$, a linear relaxation can be represented as a quadruple $(A_\ell, b_\ell, A_u, b_u)$ with $A_\ell, A_u \in \mathbb{R}^{q \times p}$, $b_\ell, b_u \in \mathbb{R}^q$ satisfying

$$A_\ell x + b_\ell \leq h(x) \leq A_u x + b_u.$$

for all x in the input domain, i.e., $x \in Z$.

Here, if h is the primitive map of some node in a computation graph, the input box Z is called the **preactivation bound** of this node. The tightness of the linear relaxation can be dependent on the preactivation bounds. Below, we give several examples of linear relaxation:

a) Affine map: For $h(x) = Mx + c$ on any box Z , the relaxation is exact:

$$A_\ell = M, \quad b_\ell = c, \quad A_u = M, \quad b_u = c. \quad (10)$$

For multi-input $h(x^{(1)}, \dots, x^{(r)}) = \sum_{j=1}^r M_j x^{(j)} + c$, use $A_\ell^{(j)} = A_u^{(j)} = M_j$ and $b_\ell = b_u = c$. This relaxation is exact.

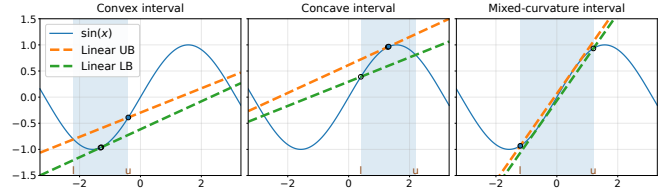


Fig. 3. Linear lower and upper bound of $h(x) = \sin(x)$.

b) Element-wise ReLU activation: Let $h(x) = \text{ReLU}(x)$ with $x \in [\ell, u]$. The linear relaxation $(A_\ell, b_\ell, A_u, b_u)$ can be chosen as

$$\text{LR}(h; [\ell, u]) = \begin{cases} (0, 0, 0, 0), & (u \leq 0), \\ (1, 0, 1, 0), & (\ell \geq 0), \\ (\alpha, 0, \frac{u}{u-\ell}, -\frac{u}{u-\ell} \ell) & (\ell < 0 < u) \end{cases} \quad (11)$$

for any $\alpha \in [0, 1]$.

c) Sin: Let $h(x) = \sin(x)$ with $x \in [\ell, u]$. Because the sine function changes convexity, the linear relaxation must be adjusted based on the range of ℓ and u . A visualization of the linear bound can be found in Figure 3. Concretely, for an interval $[\ell, u] \subset [-\pi, \pi]$, the linear relaxation is constructed as follows (relaxations for other regions are derived similarly):

- **Concave region** ($\ell \geq 0$): We use the secant line over $[\ell, u]$ as a valid lower bound, and an appropriate tangent line as an upper bound.
- **Convex region** ($u \leq 0$): We use the secant line over $[\ell, u]$ as a valid upper bound, and an appropriate tangent line as a lower bound.
- **Mixed region** ($\ell < 0 < u$): Since the interval spans both convex and concave parts, we construct both bounds using tangent lines.

d) Element-wise Multiplication: Let $h(x, y) = xy$ with $(x, y) \in [\ell_x, u_x] \times [\ell_y, u_y]$. The optimal linear relaxations are given by the McCormick envelopes, which establish two valid lower bounds and two valid upper bounds

$$\begin{aligned} xy &\geq \ell_y x + \ell_x y - \ell_x \ell_y \\ xy &\geq u_y x + u_x y - u_x u_y \\ xy &\leq \ell_y x + u_x y - u_x \ell_y \\ xy &\leq u_y x + \ell_x y - \ell_x u_y \end{aligned} \quad (12)$$

Any convex combination of the lower bounds forms a valid lower relaxation, and any convex combination of the upper bounds forms a valid upper relaxation. For instance, selecting the first lower bound and the first upper bound yields the linear relaxation

$$\text{LR}(h; [\ell_x, u_x] \times [\ell_y, u_y]) = ([\ell_y \ell_x], -\ell_x \ell_y, [\ell_y u_x], -u_x \ell_y). \quad (13)$$

We are now ready to introduce the actual backward symbolic bound propagation algorithm used in α, β -CROWN. As a motivating example of how the algorithm works to derive a bound like in equation (8), we consider a simple feed-forward neural network defined recursively as

$$\begin{aligned} F(x) &= c^\top z^n(x) \\ z^{k+1}(x) &= \text{ReLU}(W^{k+1} z^k(x)) \\ z^0(x) &= x. \end{aligned} \quad (14)$$

Assume we have a verification target of $F(x) > 0$, and that all intermediate preactivation bounds have already been computed. We start the propagation with the exact equation $F(x) = c^\top z^n(x)$. To propagate backward through the final ReLU layer, let $y^n(x) = W^n z^{n-1}(x)$ be the preactivation. From the linear relaxation in eq. (11), we can construct diagonal matrices A_ℓ^n, A_u^n and bias vectors b_ℓ^n, b_u^n such that

$$A_\ell^n y^n(x) + b_\ell^n \leq \text{ReLU}(y^n(x)) \leq A_u^n y^n(x) + b_u^n. \quad (15)$$

Because $F(x)$ is a linear combination of these ReLU outputs weighted by c , we must split c into its positive and negative components element-wise: $c^+ = \max(c, 0)$ and $c^- = \min(c, 0)$. Multiplying the relaxation by these components gives us valid bounds in terms of the preactivation $y^n(x)$

$$\underline{A}_{\text{pre}}^n y^n(x) + \underline{b}_{\text{pre}}^n \leq F(x) \leq \bar{A}_{\text{pre}}^n y^n(x) + \bar{b}_{\text{pre}}^n, \quad (16)$$

where

$$\begin{aligned} \bar{A}_{\text{pre}}^n &= (c^+)^\top A_u^n + (c^-)^\top A_\ell^n, \\ \bar{b}_{\text{pre}}^n &= (c^+)^\top b_u^n + (c^-)^\top b_\ell^n, \\ \underline{A}_{\text{pre}}^n &= (c^+)^\top A_\ell^n + (c^-)^\top A_u^n, \\ \underline{b}_{\text{pre}}^n &= (c^+)^\top b_\ell^n + (c^-)^\top b_u^n. \end{aligned} \quad (17)$$

Next, we substitute $y^n(x) = W^n z^{n-1}(x)$ to step backward through the linear layer. This yields the bounds in terms of the previous layer's post-activation $z^{n-1}(x)$:

$$\underline{A}^{n-1} z^{n-1}(x) + \underline{b}^{n-1} \leq F(x) \leq \bar{A}^{n-1} z^{n-1}(x) + \bar{b}^{n-1} \quad (18)$$

where $\bar{A}^{n-1} = \bar{A}_{\text{pre}}^n W^n$ and $\underline{A}^{n-1} = \underline{A}_{\text{pre}}^n W^n$, while the biases remain unchanged ($\bar{b}^{n-1} = \bar{b}_{\text{pre}}^n$ and $\underline{b}^{n-1} = \underline{b}_{\text{pre}}^n$).

Now we can substitute $z^{n-1}(x)$ with $\text{ReLU}(W^{n-1} z^{n-2}(x))$ and recursively continue this propagation until we reach the input x . This backward linear bound propagation naturally preserves the linear dependencies between nodes. As a result, it produces much tighter bounds compared to plain interval bound propagation (IBP), which naively pushes independent ranges forward. A full formal algorithm of this procedure is presented in Algorithm 1. For simplicity of notation, we assume that there is only one output node and one input node, but the algorithm extends to multiple input/output nodes trivially. This algorithm can terminate with theoretical guarantees as follows.

Theorem 1: When Algorithm 1 terminates, it is guaranteed that we have

$$F(x) \geq \underline{A}x + \underline{b}, \quad \forall x \in \mathcal{B} \quad (19)$$

and thus we obtain a sound lower bound of $F(x)$.

For a proof of this theorem, we refer the reader to Theorem 1 in the original `auto_liRPA` paper [49]. The algorithm requires sound linear relaxation, which in turn requires access to preactivation bounds. We note that these preactivation bounds can be obtained in several ways, where the simplest and tightest approach is to recursively apply Algorithm 1. To be more precise, for each node where we need its preactivation bound, we apply Algorithm 1 to the subgraph of G that has this specific node as output node.

Algorithm 1 Backward Linear bound propagation

Require: Computation Graph $G = (V, E)$ of $F : \mathbb{R}^n \rightarrow \mathbb{R}$; for each non-input node i a valid local relaxation $(A_{\ell,i}^{(j)}, b_{\ell,i}, A_{u,i}^{(j)}, b_{u,i})$ w.r.t. parents $j \in u(i)$ given intermediate bounds and the input domain \mathcal{B} ; output node o ; input node x

Ensure: $\underline{A} \in \mathbb{R}^{1 \times n}$, $\underline{b} \in \mathbb{R}$ with $F(x) \geq \underline{A}x + \underline{b}$ on \mathcal{B}

- 1: Set $\underline{A}_o \leftarrow 1$, $\underline{d} \leftarrow 0$; $\underline{A}_i \leftarrow 0$ for all $i \neq o$
 - 2: $\text{deg}_i \leftarrow \text{GETOUTDEGREE}(G)$
 - 3: initialize queue $Q \leftarrow [o]$
 - 4: **while** $Q \neq \emptyset$ **do**
 - 5: $i \leftarrow Q.\text{POP}()$
 - 6: **for all** $j \in u(i)$ **do**
 - 7: $\Lambda_j \leftarrow (\underline{A}_i)^+ A_{\ell,i}^{(j)} + (\underline{A}_i)^- A_{u,i}^{(j)}$
 - 8: $\underline{A}_j \leftarrow \underline{A}_j + \Lambda_j$
 - 9: $\text{deg}_j \leftarrow \text{deg}_j - 1$
 - 10: $\underline{d} \leftarrow \underline{d} + (\underline{A}_i)^+ b_{\ell,i} + (\underline{A}_i)^- b_{u,i}$
 - 11: $\underline{A}_i \leftarrow 0$
 - 12: **for all** $j \in u(i)$ **do**
 - 13: **if** $\text{deg}_j = 0$ **and** j is not input **then**
 - 14: $Q.\text{PUSH}(j)$
 - 15: **return** $\underline{A} \leftarrow \underline{A}_x$, $\underline{b} \leftarrow \underline{d}$
-

Since for each input node we already have its preactivation bound, i.e., the domain \mathcal{B} , the recursion will eventually terminate.

Intuitively, backward bound propagation is analogous to gradient backpropagation: both traverse the computation graph and repeatedly propagate a local quantity at each node. The key difference is that gradient backpropagation propagates derivatives, whereas LiRPA propagates linear upper/lower relaxations, composing them across layers to obtain a global affine bound. This propagation is computationally lightweight: its runtime is comparable to a standard backward gradient pass, simply applying a closed-form local linear relaxation in place of a gradient at each node. This efficiency makes it practical to tighten certificates by running the propagation over many sub-domains of \mathcal{B} in parallel or batch (input domain branch-and-bound), as detailed next.

From Algorithm 1, it is evident that any nonlinear node can be handled if it admits a linear relaxation that can be efficiently computed. α, β -CROWN implements many commonly used nonlinearities like ReLU, tanh, *, /, trig functions, and many others. We list some currently implemented nonlinearities in Table I.

C. Handling Jacobian

In control problems, verification tasks often require bounding not just the output of a computation graph G , but also the Jacobian of its induced function F_G . For example, analyzing the Lyapunov stability for a continuous-time system requires bounding the gradient ∇V as a function of its input state x [59]. The key idea is to extend the graph itself so that it explicitly encodes the gradient computation via the chain rule, just like the auto-differentiation. Starting from the output node, we backtrack through the graph, attaching a

TABLE I
OPERATORS SUPPORTED BY α, β -CROWN.

Category	Operators
Element-wise arithmetic & math	add, sub, mul, div; neg, pow, abs, square, reciprocal, exp, log, sqrt; sin, cos, tan, atan
Nonlinear activations	relu, hardtanh; tanh, sigmoid, gelu
Reduction	reduce_sum, reduce_mean, reduce_max; max, min
Linear / Matrix	linear; matmul
Convolutional	conv2d; conv_transpose2d
Shape manipulation	reshape, flatten; transpose; squeeze, unsqueeze; expand; concat, slice; gather
Stochastic / Regularization	dropout; softmax

corresponding “gradient node” to each operator by taking local derivatives. This augments the original computation graph with a new set of nodes and edges, forming an extended computation graph that represents the backward gradient propagation. Evaluating this extended graph directly yields the Jacobian with respect to the inputs of the original graph. The same linear relaxation-based techniques implemented in auto_LiRPA can then be applied to this extended graph, thereby producing certified bounds on the Jacobian in exactly the same manner as bounds on the original function. This procedure allows us to treat Jacobian computation as essentially another operator on the computation graph that can be handled easily.

D. Branch and Bound (BaB)

The linear bound obtained by bound propagation may be potentially conservative, in which case the affine bound may sit noticeably below F on the domain \mathcal{B} , and thus misses some verifiable cases. To mitigate this issue, α, β -CROWN can perform **input domain branch-and-bound** to dynamically partition the input domain \mathcal{B} into many small pieces $\{\mathcal{B}_i\}_{i=1}^n$. It then runs Algorithm 1 to get a lower bound of F on each of the subdomains, and uses the minimum of these lower bounds as the final certificate. Intuitively, since a function could be better approximated by linear functions under a smaller input domain, the bound we get from Algorithm 1 on each of the subdomains will be tighter. Furthermore, for a piecewise linear activation like ReLU, partitioning the domain significantly increases the likelihood of neuron stabilization (as seen in Equation (11)). The full algorithm of input branch-and-bound is detailed in Algorithm 2.

In practice, since bound propagation is very efficient and parallelizable, the efficacy of the BaB algorithm hinges on how we split each unverified domain in lines 10 and 11 of Algorithm 2. While partitioning the domain along any dimension shrinks the input space and generally improves the linear relaxation, splitting along different dimensions can yield vastly different improvements in the resulting lower bound. To this end, α, β -CROWN implements several

Algorithm 2 Input Domain Branch-and-Bound Verification

Require: function F , initial domain Ω , batch size B

- 1: $\mathcal{S} \leftarrow \text{STACK}([\Omega])$ \triangleright unverified subdomains
- 2: **while** $\mathcal{S} \neq \emptyset$ **do**
- 3: $\mathcal{B} \leftarrow \text{POPBATCH}(\mathcal{S}, B)$ \triangleright pop up to B subdomains
- 4: $\mathcal{U} \leftarrow \emptyset$
- 5: **for each** $D \in \mathcal{B}$ **do**
- 6: compute lower bounds of $F(x)$ over D
- 7: **if** $F(x) > 0$ cannot be certified on D **then**
- 8: add D to \mathcal{U}
- 9: **if** $\mathcal{U} \neq \emptyset$ **then**
- 10: **for each** $D \in \mathcal{U}$ **do**
- 11: $D_1, D_2 \leftarrow \text{SPLIT}(D)$; $\text{PUSH}(\mathcal{S}, D_1, D_2)$
- 12: **if** $\mathcal{S} = \emptyset$ **then**
- 13: **return** VERIFIED \triangleright all subdomains verified

different heuristics for the SPLIT function in line 11. Here we introduce the two most commonly used heuristics [95].

a) *Naive Branching*: In this splitting heuristic, we simply split the longest edge of the input domain \mathcal{B} . To be more precise, suppose $\mathcal{B} = \prod_{i=1}^n [\ell_i, u_i]$. We first compute $k = \arg \max_i |u_i - \ell_i|$, and split \mathcal{B} into

$$\begin{aligned} \mathcal{B}_1 &= \prod_{i \neq k} [\ell_i, u_i] \times \left[\ell_i, \frac{\ell_i + u_i}{2} \right] \\ \mathcal{B}_2 &= \prod_{i \neq k} [\ell_i, u_i] \times \left[\frac{\ell_i + u_i}{2}, u_i \right] \end{aligned} \quad (20)$$

b) *Smart Branching* [95]: This differs from the naive branching only in how the split index k is chosen. On the domain $\mathcal{B} = \prod_{i=1}^n [\ell_i, u_i]$, after the bound propagation, we get a sound affine lower bound of F satisfying

$$F(x) \geq \underline{a}^\top x + \underline{b}, \quad \forall x \in \mathcal{B} \quad (21)$$

We split the index j that satisfies

$$j = \arg \max_i |a_i| (u_i - \ell_i), \quad (22)$$

which essentially computes the most sensitive dimension that could potentially improve the bound.

In practice, we often prefer smart branching over naive branching, although it does not always guarantee improvements. Thanks to the efficiency of the bound-propagation algorithm (1), which can be done on GPUs, we can acceptably divide the domain \mathcal{B} into tens of thousands of pieces. Furthermore, α, β -CROWN implements efficient parallelization that effectively computes bounds on these divided domains simultaneously. After repeated branching, each domain will be tiny, and the linear over-approximation will often be tight enough to enable verification. This provides the main intuitive idea on how α, β -CROWN achieves state-of-the-art verification results on problem (5).

E. Supporting General Satisfiability Problems

Up to now, we have focused on obtaining tight numeric and linear bounds for formulas like (5). In practice, when we solve satisfiability problems, specifications are often more complex and involve logical combinations of multiple

constraints, just like the motivating example of Lyapunov stability in Section II. Thanks to the parallelizable nature of bound propagation and the flexibility of the branch and bound procedure, α, β -CROWN can naturally handle such cases. In principle, α, β -CROWN can handle many cases that a traditional SMT solver for real numbers, such as dReal, can handle, and in a much more scalable fashion. Here we discuss how α, β -CROWN handles the following three typical forms.

1) *Multiple OR constraints*: An OR specification requires at least one of several conditions to hold:

$$F_1(x) > 0 \vee F_2(x) > 0 \vee \dots \vee F_k(x) > 0. \quad (23)$$

To encode this efficiently, we exploit the fact that all operations in α, β -CROWN are vectorized. A linear transformation on the final layer can re-parameterize the outputs into

$$\tilde{F}(x) \succ_{\vee} 0, \quad (24)$$

where verification succeeds if any entry of $\tilde{F}(x)$ is positive (i.e., $\max_i \tilde{F}_i(x) > 0$). In other words, all disjunctions are checked in parallel as components of a tensor.

Example 2 (Implication): Suppose we want to verify a simple implication: $A(x) \rightarrow B(x)$. For instance:

- If the state is inside a “trigger region” $A(x) : \|x\| \leq 1$,
- then the system must satisfy a safety condition $B(x) : g(x) \leq 0$.

This is equivalent to checking

$$(\|x\| > 1) \vee (g(x) \leq 0). \quad (25)$$

In α, β -CROWN, this can be written in the form as

$$\tilde{F}(x) = \begin{bmatrix} \|x\| - 1 \\ -g(x) \end{bmatrix} \succ_{\vee} 0 \quad (26)$$

The bound of $\tilde{F}(x)$ above is computed in vector form. At any stage of the algorithm, if for a subdomain \mathcal{B} the propagated bound already certifies $\tilde{F} \succ_{\vee} 0$, then the subdomain is considered verified. A real example of the implication type constraints is given in Section IV.

2) *Multiple AND constraints*: An AND specification requires *all* constraints to hold simultaneously:

$$F_1(x) > 0 \wedge F_2(x) > 0 \wedge \dots \wedge F_k(x) > 0. \quad (27)$$

In α, β -CROWN, each conjunct is considered separately. During BaB, all of them are added to the domain stack \mathcal{S} . Verification succeeds only when every conjunct has been individually certified (i.e., removed from the stack). The example in Section II is a real application of multiple AND constraints.

3) *General Boolean specification*: More complex specifications may mix AND and OR operators. For example,

$$(F_1(x) > 0 \vee F_2(x) > 0) \wedge (F_3(x) > 0) \vee (F_4(x) > 0). \quad (28)$$

Such formulas can always be rewritten in conjunctive normal form (CNF): a conjunction of clauses, each of which is a disjunction. Each disjunctive clause can be handled as in case (1), and the outer conjunction is treated as in case (2).

F. Overall Pipeline for Solving Satisfiability Problems

The α, β -CROWN framework is designed to be flexible. In principle, multiple verifiers and falsifiers can be composed in different orders, depending on the verification target and efficiency considerations. However, in typical control problems, we often follow a practical pipeline that balances speed and completeness. The pipeline is illustrated in Figure 4.

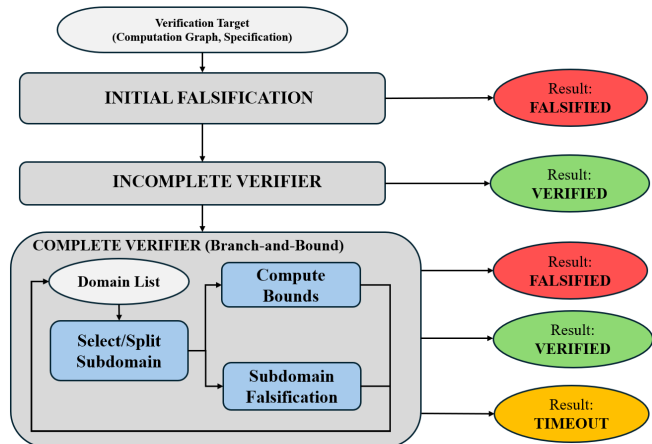


Fig. 4. Overview structure of α, β -CROWN

1) *Initial Falsification*: The process begins with a falsifier, where we typically apply a projected gradient descent (PGD) [96] to search for counterexamples to the verification condition. Concretely, PGD performs gradient-based minimization on the violation objective (e.g., the margin in (5)) over a large batch of initial candidates, and after each step projects the candidates back onto the allowed input set. If a violating input $x \in \mathcal{B}$ is found such that the specification fails, the procedure terminates immediately with falsification.

2) *Incomplete verifier (bound propagation with no BaB)*: If no counterexample is found, we proceed with an incomplete verifier, which consists of a simple bound propagation pass with no branch-and-bound. This step computes sound but possibly conservative bounds with auto_LiRPA.

- If the bounds already certify the property, the procedure stops here and returns verification.
- Otherwise, the bounds provide initialization for the complete verifier, for example, intermediate layer pre-activation bounds.

3) *Complete verifier (branch-and-bound)*: Finally, if the incomplete verifier is inconclusive, we use a complete verifier based on input domain branch-and-bound as described in Section III-D. The input domain is recursively partitioned into subdomains, and sound affine bounds are propagated on each of them. Verification succeeds once every subdomain has been refined sufficiently so that its propagated bounds alone can certify the property. In the meantime, during branch-and-bound, since the domain becomes smaller, counterexamples might be easier to locate. Therefore, we also perform a more fine-grained falsification on each subdomain during branch-and-bound to ensure that no counterexamples

are missed. In practice, branch-and-bound runs under some budget, like a predefined time limit. If the budget is exhausted before the verifier can prove or refute the property, an inconclusive result is returned.

IV. APPLICATIONS TO CONTROL

In this section, we provide several applications of using α, β -CROWN in the control setting. In particular, since casting control certificates into a satisfiability form is often the most subtle step, we focus on the corresponding problem reformulations. We shall discuss how to use it to verify the stability certificate, safety certificate, and contraction.

Throughout this section, we consider either a closed-loop discrete-time system:

$$x_{t+1} = f(x_t, \pi(x_t)) = g(x_t), \quad (29)$$

or a closed-loop continuous system

$$\dot{x} = f(x, \pi(x)) = g(x). \quad (30)$$

We denote the solution of this system with initial condition $x_0 = x$ as $\phi(t, x)$. In what follows, we assume that the controller $u(\cdot)$ and corresponding certifications, such as Lyapunov function or contraction metrics, are given and focus exclusively on verification. We defer all details on how to co-learn the controller with a formal certificate to the next section. Furthermore, we assume that f, π are general computation graphs with nonlinearities being those presented in Table I that are supported by α, β -CROWN.

A central challenge in applying α, β -CROWN to control tasks is to make the classical certificate checkable by a verifier that only supports box input domains. For example, since the traditional Lyapunov theory and barrier function theory need forward invariance, they are naturally stated on implicitly defined sets such as the sublevel set $\Omega_\rho^V = \{x : V(x) \leq \rho\}$, whereas α, β -CROWN can only verify conditions in a box domain \mathcal{B} . The naive workaround, which is to verify the decrease condition over the entire box \mathcal{B} and then locate the maximal invariance set inside it, is typically overly conservative and is likely to fail even when a valid certificate exists. Therefore, we instead rewrite each certificate as an implication on the sublevel set, and then convert it into an equivalent satisfiability condition over the surrounding box. In the following sections, we shall demonstrate in detail how to reformulate classical control certificates, including discrete-time and continuous-time Lyapunov analysis, continuous-time barrier function, and discrete-time contraction analysis, into verifier-friendly constraints over a box domain.

A. Reachability Analysis

Before we dive into the actual certification criterion with α, β -CROWN, we shall first briefly discuss how to use the bound produced by auto_LiRPA to conduct reachability analysis for a discrete-time system. Reachability analysis asks: given an initial set of states X_0 and a closed-loop dynamics map $g(x) = f(x, \pi(x))$, what set of states can the system reach after one or multiple time steps? The

reachable set computed can be used by downstream tasks, such as safety verification over a finite horizon. In general, exactly computing $X_{t+1} = g(X_t)$ is intractable for nonlinear dynamics and neural-network controllers. Instead, we aim to compute a sound over-approximation $\widehat{X}_{t+1} \supseteq g(X_t)$ that is cheap to obtain but guaranteed to contain all successors. auto_LiRPA provides exactly this capability: by treating g as a computation graph and X_t as an input domain (typically a box or a polytope), it can certify elementwise bounds on $g(x)$ for all $x \in X_t$, which directly yields a sound reachable set over-approximation, and iterating this one-step over-approximation produces a forward reachable tube.

B. Discrete-Time Lyapunov Analysis

The goal of stability analysis is to certify that the controller $\pi(\cdot)$ stabilizes the systems in (29) and (30), and to characterize the domain of initial states from which trajectories are guaranteed to converge to the equilibrium. Formally, we aim to find the region of attraction (ROA) of the system, defined as follows.

Definition 3 (Region of Attraction (ROA) [93]): Region of attraction for the system (29) or (30) is the set \mathcal{R} such that $\lim_{t \rightarrow \infty} \phi(t, x_0) = x^*$ for all $x_0 \in \mathcal{R}$.

In practice, Lyapunov theory is the standard tool to certify such guarantees: one seeks a scalar “energy” function V whose value decreases along closed-loop trajectories, so that the trajectories from a forward invariant set converge to the equilibrium, yielding an inner approximation of the ROA [94]. We now state a Lyapunov-based theorem that formalizes this certification criterion that can be used by α, β -CROWN. We first start with discrete-time systems [57].

Theorem 2 (Lyapunov Theorem (Discrete-Time) [97]):

Given a forward invariant set \mathcal{S} containing the equilibrium, if there exists a function $V : \mathcal{S} \rightarrow \mathbb{R}$ such that we have

$$\begin{aligned} V(x^*) &= 0 \\ V(x) &> 0 \quad (\forall x \in \mathcal{S} \setminus \{x^*\}) \\ V(g(x_t)) - V(x_t) &\leq -\kappa V(x_t) \quad (\forall x_t \in \mathcal{S}) \end{aligned} \quad (31)$$

for some $\kappa > 0$, then \mathcal{S} is a subset of the region of attraction for the discrete-time system (29).

Now suppose we have synthesized a candidate V through learning or other means, and would like to formally verify its correctness with α, β -CROWN. As the verifier can only handle a box input, we begin by fixing a box-shaped region of interest \mathcal{B} containing the equilibrium state x^* and constraining the forward invariant set \mathcal{S} to be the intersection of the box \mathcal{B} with a sublevel set of V , as

$$\mathcal{S} := \{x \in \mathcal{B} \mid V(x) < \rho\} \quad (32)$$

for some $\rho > 0$ that ensures for any $x \in \mathcal{S}$, we have $x_{t+1} \in \mathcal{B}$. Clearly, by the sublevel set structure, if the Lyapunov function values are certified to decrease along the trajectory, x_{t+1} will also land in \mathcal{S} , making \mathcal{S} forward invariant. Therefore, we reach the following verification condition.

Discrete-Time System Stability Verification

Theorem 3: Suppose that $V(x^*) = 0$ and V is positive everywhere else. Let $F(x) := V(g(x)) - (1 - \kappa)V(x)$. If the condition

$$(-F(x) \geq 0 \wedge g(x) \in \mathcal{B}) \vee (V(x) \geq \rho), \quad \forall x \in \mathcal{B} \quad (33)$$

holds for some $\rho > 0$, then \mathcal{S} is a certified ROA inner-approximation for the closed-loop system (29).

Proof: By theorem 2, we just need to check that \mathcal{S} is forward invariant and the Lyapunov function decreases along trajectories for any trajectories in \mathcal{S} . We take any $x \in \mathcal{S}$. Then $x \in \mathcal{B}$ and $V(x) < \rho$. Therefore, we know that $g(x) \in \mathcal{B}$ and $V(g(x)) \leq (1 - \kappa)V(x) < \rho$. Therefore, $g(x) \in \mathcal{S}$ and \mathcal{S} is forward invariant. The above analysis also shows that the Lyapunov function values decrease along trajectories in \mathcal{S} . ■

Now, since the verification condition (33) is on a box \mathcal{B} , and all the conditions can be cast into scalar value inequalities, it can be directly handled by α, β -CROWN as described in the general specification section III-E.

C. Continuous-Time Lyapunov Analysis

For continuous-time systems, the essence is similar [59]. To present the verification criterion, we first state the continuous-time Lyapunov theorem.

Theorem 4 (Lyapunov Theorem (Continuous-Time) [94]): Given a forward invariant set \mathcal{S} containing the equilibrium, if there exists a function $V : \mathcal{S} \rightarrow \mathbb{R}$ such that we have

$$\begin{aligned} V(x^*) &= 0 \\ V(x) &> 0 \quad (\forall x \in \mathcal{S} \setminus \{x^*\}) \\ \nabla V(x)f(x, \pi(x)) &\leq -\kappa V(x) \quad (\forall x \in \mathcal{S}) \end{aligned} \quad (34)$$

for some $\kappa > 0$, then \mathcal{S} is a subset of the region of attraction for the continuous-time system (30).

We note that this differs from the discrete-time Lyapunov theorem in the sense that it requires the differentiability of the function V , and the decrease condition is now formalized with a differential change rather than a discrete change. This makes it more difficult to parametrize V to satisfy the positive definiteness condition directly when we wish to use a neural network based parametrization. Therefore, in practice, we exclude the verification on a small neighborhood around the origin. Moreover, the forward invariance condition in continuous-time theory is trickier than in the discrete-time counterpart. We must ensure that, on the intersection of the ROA boundary and the box boundary, the closed-loop vector field points inward so that trajectories cannot escape the box. In conclusion, the verification condition can be encoded in the following theorem.

Theorem 5 ([61]): Let $0 < c_1 < c_2$. We denote $V^{\leq c} := \{x : V(x) \leq c\}$ and $V^{\leq c_2} \setminus \leq c_1 := V^{\leq c_2} \setminus V^{\leq c_1}$. Suppose we have

$$x \in V^{\leq c_2} \setminus \leq c_1 \cap \mathcal{B} \implies \nabla V(x) \cdot f(x, \pi(x)) \leq -\kappa V(x), \quad (35)$$

$$x \in \partial \mathcal{B} \cap V^{\leq c_2} \implies f(x, \pi(x)) \cdot \bar{n}(x) \leq 0, \quad (36)$$

where $\bar{n}(x)$ is the outer normal vector of $\partial \mathcal{B}$ at x . Then both $V^{\leq c_1}$ and $V^{\leq c_2}$ are *forward invariant*, and every trajectory initialized in $V^{\leq c_2}$ enters the smaller set $V^{\leq c_1}$ in finite time.

To convert this condition into a form that α, β -CROWN can verify, again, we need the verification to happen on the box domain \mathcal{B} . Formally, it can be converted into the following criterion.

Continuous-Time System Stability Verification

Theorem 6: Let $F(x) := \nabla V(x) \cdot f(x, \pi(x)) + \kappa V(x)$ and $G(x) := f(x, \pi(x)) \cdot \bar{n}(x)$. The above theorem is equivalent to verifying

$$(F(x) \leq 0) \vee (V(x) > c_2) \vee (V(x) < c_1) \quad (37)$$

$$(G(x) \leq 0) \vee (x \notin \partial \mathcal{B}) \vee (V(x) > c_2) \quad (38)$$

for all $x \in \mathcal{B}$. Moreover, we shall see that since \mathcal{B} is a box domain, the condition $x \in \partial \mathcal{B}$ can be easily converted into several numerical conditions.

Since in practice the sublevel set $\{x : V(x) \leq c_1\}$ is small, this theorem essentially proves that $\{x : V(x) \leq c_2\}$ is an inner approximation of the ROA. Now both conditions (37) and (38) can be verified by α, β -CROWN using the strategy discussed in Section III-E.

D. Robust Control under Disturbance and Uncertainty

In this section, we consider generalized systems with exogenous inputs

$$x_{t+1} = f(x_t, \pi(x_t), w_t) = g(x_t, w_t). \quad (39)$$

We wish to find a robust forward invariant set under all possible disturbances, and to achieve this, we would need a generalized Lyapunov function. Let's consider the case where the disturbances w_t are bounded pointwise by $\phi(w_t) \leq v$. In this case, the following theorem provides a sufficient condition that is compatible with α, β -CROWN.

Theorem 7 (Uniform Disturbance Robustness): Let $\mathcal{B} \times \mathcal{B}^w \subset \mathbb{R}^n \times \mathbb{R}^{n_w}$ be a box constrained set containing $(0, 0)$ and $V : \mathbb{R}^n \rightarrow \mathbb{R}$ be a continuous positive-definite function. Suppose that the admissible set of disturbances given by a constraint function $\psi : \mathbb{R}^{n_w} \rightarrow \mathbb{R}$ and $v > 0$ is non-empty

$$\mathcal{W} := \{w : w_k \in \mathcal{B}^w, \psi(w_k) \leq v, \forall k\} \quad (40)$$

which defines the following product domain:

$$\mathcal{S}_\rho^V := \{(x, w) \in (\Omega_\rho^V \cap \mathcal{B}) \times \mathcal{B}^w : \psi(w) \leq v\} \quad (41)$$

and suppose that the following holds for some $\kappa \in (0, 1)$:

$$\mathcal{S}_\rho^V \subseteq \{(x, w) : f(x, w) \in \mathcal{B}, F_V(x, w) \leq 0\}, \quad (42)$$

where $F_V(x, w) = V(f(x, w)) - (1 - \kappa)V(x) - \psi(w)$. If $v/\kappa \leq \rho$, $x_0 \in \mathcal{X} := \Omega_\rho^V \cap \mathcal{B}$ and $w \in \mathcal{W}$, then the solution to (39) satisfies $(x_k, w_k) \in \mathcal{S}_\rho^V$ for all k . Furthermore, if there is no disturbance and $w = 0$ and $\psi(0) \leq 0$, then $\Omega_\rho^V \cap \mathcal{B}$ is a forward-invariant subset of the ROA.

This result shows that if the change in $V(x_k)$ can be bounded at each step by a known function $\psi(w_k)$, and if

this bound stays within a fraction κ of the energy level ρ , then the trajectory remains within the sublevel set Ω_ρ^V . Given a candidate storage function V and the constraint function ψ , Theorem 7 can be directly verified by α, β -CROWN with the following specification:

Discrete-Time systems Stability Verification with Uniform Bounded Disturbance

$$(F_V(x, w) \leq 0 \wedge f(x, w) \in \mathcal{B}) \vee (V(x) > \rho) \vee (\psi(w) > \nu) \quad (43)$$

by checking all $(x, w) \in \mathcal{B}^x \times \mathcal{B}^w$. A similar theorem can be derived to handle integral-constrained disturbances.

E. Contraction Metrics

We further discuss how to convert the verification criterion for contractions into forms that can be tackled by α, β -CROWN. Traditionally, discrete-time contraction conditions are usually expressed as matrix inequalities [98], which are difficult for scalar-valued verifiers to handle and also rely on differentiability of the dynamics. Therefore, we propose to reformulate the contraction condition into a scalar satisfiability problem as follows.

Theorem 8 (Contraction [59]): Assume that \mathcal{X} is an open, connected, and forward invariant subset in \mathbb{R}^n , and the dynamics f is continuous. Given a positive threshold $\varepsilon > 0$, suppose there exists uniformly continuous $M(x) : \mathcal{X} \rightarrow \mathbb{S}_{++}^{n \times n}$ with a uniform lower bound $\mu I \preceq M(x)$ that satisfies

$$\sqrt{(f(x) - f(y))^\top M(f(x))(f(x) - f(y))} \leq \rho \sqrt{(x - y)^\top M(x)(x - y)} \quad (44)$$

for all $x \in \mathcal{X}$ and $y \in \mathcal{B}(x; \varepsilon) \cap \mathcal{X}$ and some $0 < \rho < 1$, then the system (29) is contracting with respect to the Riemannian metric d induced by M , i.e, the system satisfies

$$d(f(x), f(y)) \leq \rho d(x, y) \quad (45)$$

for any $x, y \in \mathcal{X}$.

This condition can now be written in a form that is compatible with α, β -CROWN, and the assumption is reduced to only assuming the continuity of the closed-loop dynamics, which can incorporate many neural-controlled systems. The forward invariant domain \mathcal{X} can be found with Lyapunov sublevel sets or through condition (33). Assuming we have already obtained such an invariant set, the contraction condition can be formulated as follows. We note that here the technique to transform the verification condition on the complex forward invariant set into a box is essentially the same as in the Lyapunov setting. Formally, the satisfiability problem to be solved can be defined as follows.

Discrete-Time System Contraction Analysis

Theorem 9: Suppose we have already formally verified the forward invariance of

$$\mathcal{X} := \{x : V(x) < \rho\} \cap \mathcal{B}.$$

For $(x, \delta) \in \mathcal{B} \times [-\varepsilon, \varepsilon]^n$, define

$$\Delta_f(x, \delta) := f(x + \delta) - f(x),$$

and

$$G(x, \delta) := \Delta_f(x, \delta)^\top M(f(x)) \Delta_f(x, \delta) - \rho^2 \delta^\top M(x) \delta.$$

Assume that, for all $(x, \delta) \in \mathcal{B} \times [-\varepsilon, \varepsilon]^n$,

$$(x + \delta \in \mathcal{B}) \wedge (V(x) < \rho) \wedge (V(x + \delta) < \rho) \implies G(x, \delta) \leq 0. \quad (46)$$

Then the system (29) is certifiably contracting on \mathcal{X} with contraction rate $\rho' \in (\rho, 1)$.

F. Barrier Function

We further consider a safety certificate with barrier functions [77]. In this setting, we wish to prove the forward invariance of a safe set C of the following form:

$$C = \{x \in \mathbb{R}^n : h(x) \geq 0\}, \quad (47)$$

$$\partial C = \{x \in \mathbb{R}^n : h(x) = 0\}, \quad (48)$$

$$\text{Int}(C) = \{x \in \mathbb{R}^n : h(x) > 0\}, \quad (49)$$

where h is a continuously differentiable function. The forward invariance of C can then be certified if h is a zeroing barrier function on some box \mathcal{D} with $C \subseteq \mathcal{D}$, i.e. it satisfies:

$$\nabla h(x) \cdot f(x, \pi(x)) \geq -\alpha h(x), \quad \forall x \in \mathcal{D} \cap \{h(x) \geq 0\} \quad (50)$$

for some $\alpha > 0$. This condition can then be directly verified by α, β -CROWN. More generally, we consider the control barrier function setting. Specifically for this setting, we consider a control-affine system:

$$\dot{x} = f(x) + g(x)u, \quad (51)$$

where the u can take values from a compact convex polytope $U \subset \mathbb{R}^m$. h is called a control barrier function if it satisfies

$$\sup_{u \in U} [\nabla h(x) \cdot f(x) + (\nabla h(x) \cdot g(x))u] \geq -\alpha h(x), \quad (52)$$

$\forall x \in \mathcal{D} \cap \{h(x) \geq 0\}$. As the left-hand side is linear in u , the supremum over u can be converted to a maximum over the vertices of the convex polytope U , which can then be directly verified by α, β -CROWN. Formally, we get the following verification criterion:

Continuous-Time Barrier Function Verification

Theorem 10: Let $\mathcal{D} \supseteq C$ be a box, and let $\mathcal{V}(U)$ denote the set of vertices of U . Define

$$B_h(x) := \max_{u \in \mathcal{V}(U)} [\nabla h(x)^\top f(x) + (\nabla h(x)^\top g(x))u] + \alpha h(x).$$

Then $h : \mathcal{D} \rightarrow \mathbb{R}$ is a control barrier function if and only if, for all $x \in \mathcal{D}$,

$$B_h(x) \geq 0 \vee h(x) < 0. \quad (53)$$

V. USAGE OF α, β -CROWN

The α, β -CROWN solver provides a unified, high-level entry point for working with neural networks in control and analysis tasks. Regardless of the task, the workflow consistently follows four main steps:

- 1) **Computation Graph:** Define the system dynamics and neural network as a PyTorch Module. To ensure compatibility with the solver, the graph must adhere to the following rules:
 - **Single Tensor Output:** The module must return exactly one tensor output, whose bounds will be computed. If multiple outputs are needed, they must be concatenated into a single tensor.
 - **Batch Dimension:** Each input must include a leading *batch dimension*, which should not be modified within the function.
- 2) **Variables and Solver Initialization:** Define symbolic input and output variables (e.g., `input_vars`, `output_vars`) that match the dimensions of your computation graph, and instantiate the `ABCrownSolver`.
- 3) **Constraints:** Formulate the input domain and property targets using the `IOConstraints` Domain-Specific Language (DSL).
- 4) **Execution:** Call the appropriate function for your mode (`verify()`, `compute_bounds()`, or `minimize()/maximize()`) passing the defined constraints.

To see how these steps come together in practice, it is helpful to first understand the three primary ways to use the solver:

- **Verification:** This mode mathematically proves whether a specific logical property (such as safety or stability) strictly holds across an entire continuous set of inputs.
- **Bound Computation:** Instead of answering a yes/no verification question, this mode calculates the guaranteed numerical lower and upper bounds of the computation graph’s outputs for a given input domain. This is particularly useful for finding reachable sets.
- **Optimization:** This mode runs constrained optimization directly over the input domain to find a specific input that minimizes or maximizes an objective. It returns the optimal objective value (primal value) and the corresponding input that achieves it. The solver simply uses CROWN’s bounding capabilities internally to efficiently guide the search for this optimal solution.

We will illustrate the usage with the following examples.

A. Verification Mode: Lyapunov Stability

In verification mode, the solver attempts to mathematically prove that a specific property holds across an entire continuous input domain. For a system like the Van der Pol oscillator, we can use this mode to verify its neural Lyapunov stability [61].

The condition for stability is that if the state x is within a specific level set shell $c_1 \leq V(x) \leq c_2$, then its time derivative $\dot{V}(x)$ must be strictly negative. The implication

condition can be converted into an equivalent disjunction as in condition (37). With the mathematical formulation clear, our first practical step is to implement the computation graph that represents this system.

1) *Computation Graph:* The graph takes the state, computes $V(x)$, calculates the control action, and simulates the dynamics. Note that `dynamics`, `controller`, and `lyapunov` passed into this graph are all expected to be pre-defined PyTorch Modules. To evaluate the derivative $\dot{V}(x)$ for this specific system, we need to compute the Jacobian $\nabla V(x)$. Instead of using standard auto-differentiation, the graph imports a specialized `JacobianOP` from `auto_LiRPA`. When sent to the bound computation function internally, `auto_LiRPA` automatically extends the computation graph with explicit “gradient nodes” that encode the backward gradient propagation, allowing the solver to rigorously bound the derivative.

```

1 import torch
2 import torch.nn as nn
3 from auto_LiRPA.jacobian import JacobianOP
4
5 class LyapunovComputationGraph(nn.Module):
6     def __init__(self, dynamics, controller,
7                 lyapunov):
8         super().__init__()
9         # dynamics, controller, and lyapunov
10        are all PyTorch Modules
11        self.dynamics = dynamics
12        self.controller = controller
13        self.lyapunov = lyapunov
14
15    def forward(self, x):
16        x = x.clone().requires_grad_(True)
17        V_x = self.lyapunov(x)
18        u = self.controller(x)
19        x_dot = self.dynamics(x, u)
20
21        # Define the Jacobian operator;
22        auto_LiRPA expands this internally
23        dVdx = JacobianOP.apply(V_x, x).squeeze(
24            1)
25        V_dot = torch.sum(dVdx * x_dot, dim=1,
26                          keepdim=True)
27
28        # Rule 1: Return a single concatenated
29        tensor
30        return torch.cat((V_x, V_dot), dim=1)
31
32 computation_graph = LyapunovComputationGraph(
33     dynamics, controller, lyapunov)

```

2) *Variables and Solver Initialization:* We declare variables matching the dimensions of the state input and the stacked output conditions, then tie them to the computation graph by initializing the solver.

```

1 from abcrown import (
2     ABCrownSolver, ConfigBuilder, IOConstraints
3     , input_vars, output_vars
4 )
5 # Note: These imports are needed for all the
6 # following examples.
7 # 2. Define graph input and output variables
8 x = input_vars(2) # State vector

```

```

8 y = output_vars(2) # y[0] = V(x), y[1] = V_dot(
  x)
9
10 # 3. Create solver instance with the
  computation graph
11 cfg = ConfigBuilder.from_defaults()
12
13 solver = ABCrownSolver(computation_graph, x, y,
  config=cfg)

```

3) *Constraints*: Now that the variables are ready, we need to formalize the input limits and the property we want to verify using `IOConstraints`. Note that the API strictly requires output constraints to use `<` or `>`, not `<=` or `>=`.

```

1 # 4. Create verification constraints
2 input_constraints = (x >= [-4.8, -10.8]) & (x
  <= [4.8, 10.8])
3
4 # Translate: V(x) < c1 OR V(x) > c2 OR V_dot(x)
  < 0
5 c1, c2 = 0.1, 2.0
6 output_constraints = (y[0] < c1) | (y[0] > c2)
  | (y[1] < 0.0)
7
8 constraints = IOConstraints(
9   input_vars=x, output_vars=y,
10  input_constraints=input_constraints,
11  output_constraints=output_constraints
12 )

```

4) *Execution*: Finally, we run the verification by passing the constraints to the solver.

```

1 # 5. Run verification
2 result = solver.verify(constraints=constraints)
3
4 print(f"Status: {result.status}, Verified: {
  result.success}")

```

B. Bound Computation Mode: One-Step Reachability

Instead of a Boolean yes/no verification, we can use the solver to directly extract guaranteed bounds on a network’s outputs under a bounded input domain. This is highly applicable for tasks like one-step reachability analysis, where we want to bound the next state of a system x_{t+1} given that the current state x_t lies within a known hyperrectangle \mathcal{B}_t .

Given discrete-time dynamics $x_{t+1} = f(x_t)$, if $x_t \in [x_{\min}, x_{\max}]$, bound computation finds tight bounds $x_{t+1, \min}$ and $x_{t+1, \max}$ such that:

$$x_{t+1} \in [x_{t+1, \min}, x_{t+1, \max}] \quad (54)$$

1) *Computation Graph*: Just like in verification, we start by defining the system. Here, we use a simple graph that wraps the neural network transition dynamics.

```

1 class ReachabilityGraph(nn.Module):
2   def __init__(self, nn_dynamics):
3     super().__init__()
4     self.nn_dynamics = nn_dynamics
5
6   def forward(self, x_t):
7     # x_t shape: [batch, 2]. Output
  represents x_{t+1}

```

```

8         return self.nn_dynamics(x_t)
9
10 computation_graph = ReachabilityGraph(
  nn_dynamics).eval()

```

2) *Variables and Solver Initialization*: We define the symbolic variables corresponding to the graph’s inputs and outputs, and use them to initialize the solver. By default, the solver iteratively refines its computed bounds using branch-and-bound until it reaches a standard timeout of 360 seconds. Often, however, users do not require extremely tight bounds and prefer to avoid long waiting times. To balance execution time with bound tightness, we can easily customize the configuration by limiting the execution time or the number of refinement steps. In this example, we reduce the timeout to 30 seconds and cap the maximum number of iterations at 100. It is also worth noting that setting “bab/max.iterations” to 1 will bypass the branch-and-bound refinement entirely, quickly yielding the naive CROWN bound.

```

1 # 2. Define graph input and output variables
2 x = input_vars(2)
3 y = output_vars(2)
4
5 # 3. Create solver instance with the
  computation graph
6 cfg = (
7   ConfigBuilder.from_defaults()
8   .set("bab/timeout", 30)
9   .set("bab/max_iterations", 100)
10 )
11 solver = ABCrownSolver(computation_graph, x, y,
  config=cfg)

```

3) *Constraints*: For bounding, we only need to define the input domain. If no output constraint is provided, the solver defaults to computing the concrete upper and lower bounds of the objective.

```

1 # 4. Create input constraints
2 # Define the set of possible current states
3 input_constraints = (x >= [-1.0, -1.0]) & (x <=
  [1.0, 1.0])
4
5 constraints = IOConstraints(
6   input_vars=x,
7   input_constraints=input_constraints
8 )

```

4) *Execution*: Next, we invoke the solver by calling `.compute_bounds()`. By default, the solver will only calculate and return the guaranteed concrete numerical bounds for the outputs.

```

1 # 5. Compute bounds on y given constraints on x
2 # Default behavior: Returns a BoundsResult
  containing only lower and upper
3 bounds_result = solver.compute_bounds(
4   constraints=constraints,
5   objective=y
6 )
7

```

```

8 print("Next state lower bounds:", bounds_result
      .lower)
9 print("Next state upper bounds:", bounds_result
      .upper)

```

Additionally, `compute_bounds()` can optionally provide the linear relaxation coefficients for the computation graph, which is incredibly useful for linearizing network dynamics in some downstream control tasks.

By passing the argument `return_linear_bounds` as `True`, the returned `BoundsResult` object will also include a `linear_bounds` variable. This returned object contains the matrices A and vectors b that define the linear bounds:

$$A_l x + b_l \leq f(x) \leq A_u x + b_u \quad (55)$$

By extracting these terms, users can explicitly reconstruct the linear relaxations.

```

1 # Pass return_linear_bounds=True to extract
  relaxation terms
2 bounds_result_with_linear = solver.
  compute_bounds(
3   constraints=constraints,
4   objective=y,
5   return_linear_bounds=True
6 )
7
8 if bounds_result_with_linear.linear_bounds is
  not None:
9   print("Linear relaxation successfully
  computed!")

```

C. Optimization Mode: Model Predictive Control (MPC)

The API allows for constrained optimization, allowing you to maximize or minimize a linear objective expression directly over the input domain while strictly enforcing constraints on both the inputs and the network's outputs.

As an example, in a single-step Model Predictive Control (MPC) problem, we aim to find the optimal control action u^* that minimizes a specific cost while respecting actuator limits and safety boundaries on the resulting state.

Suppose our system outputs the next state $x_{t+1} \in \mathbb{R}^2$. We want to minimize a linear combination of the next state's variables:

$$\min_u x_{t+1,1} + 0.5x_{t+1,2} \quad (56)$$

subject to the system dynamics, the input actuator limits, and a safety constraint ensuring the first dimension of the next state does not exceed a threshold:

$$\begin{aligned} x_{t+1} &= f(x_t, u) \\ -5 &\leq u \leq 5 \end{aligned} \quad (57)$$

$$x_{t+1,1} < 2.0$$

1) Computation Graph: Once again, we build the graph to represent the forward pass. The graph takes the control input u and returns the simulated next state x_{t+1} . The initial state x_t is treated as a constant inside the graph.

```

1 class MPCGraph(nn.Module):
2     def __init__(self, dynamics, x_current):
3         super().__init__()

```

```

4         self.dynamics = dynamics
5         self.x_current = x_current
6
7     def forward(self, u):
8         # Simulate next state
9         x_next = self.dynamics(self.x_current,
10                                u)
11
12         # Return next state (shape [batch, 2])
13         return x_next
14 computation_graph = MPCGraph(dynamics, x_t).
15     eval()

```

2) Variables and Solver Initialization: We declare u as an input variable and bind it to the solver along with the output y .

```

1 # 2. Define graph input and output variables
2 u = input_vars(1)
3 y = output_vars(2) # y represents the next
  state x_{t+1}
4
5 # 3. Build the solver
6 solver = ABCrownSolver(computation_graph, u, y)

```

3) Constraints: With the system dynamics defined, we set both the input limits and the output safety constraints.

```

1 # 4. Create constraints
2 # Actuator limits constraint (Input)
3 input_constraints = (u >= -5.0) & (u <= 5.0)
4
5 # Safety constraint on the next state (Output)
6 output_constraints = (y[0] < 2.0)
7
8 constraints = IOConstraints(
9     input_vars=u, output_vars=y,
10    input_constraints=input_constraints,
11    output_constraints=output_constraints
12 )

```

4) Execution: To execute the optimization, we call `.minimize()`. We can pass a composite linear expression of the outputs to serve as our objective.

```

1 # 5. Minimize the objective
2 # Define the objective as a linear expression
  of the outputs
3 objective_expr = y[0] + 0.5 * y[1]
4
5 # Returns OptimizationResult
6 result = solver.minimize(
7     objective=objective_expr,
8     constraints=constraints
9 )
10
11 if result.success:
12     print(f"Optimal objective value (Primal
13           Value): {result.primal_value}")
14     print(f"Optimal control action (u*): {
15           result.x_best}")

```

Note that the solver requires the objective expression to be a linear combination of the defined variables. If the objective is nonlinear (e.g., a quadratic cost $x_{t+1}^\top Q x_{t+1}$, the solution is simple: merge the formula to compute that nonlinear

objective directly into the computation graph so that it is returned as an additional output dimension. You can then specify that single output dimension as the one to minimize or constrain.

D. Satisfiability Mode: dReal-Like API

In addition to the standard verification and optimization modes using explicit PyTorch computation graphs, α, β -CROWN also provides a drop-in compatibility layer for the dReal Python API. While all SMT problems can be solved using α, β -CROWN’s native API, users who are already familiar with using traditional SMT tools can easily use this dReal-like interface.

Users with existing dReal scripts can utilize α, β -CROWN’s solver engine without rewriting their constraint definitions or learning the new API. By simply changing the import statement, the solver seamlessly processes the standard Variable, And, and CheckSatisfiability commands. Here is an example demonstrating this exact 1-to-1 compatibility:

```

1 # Simply replace 'from dreal import *' with the
  abcrown compatibility layer
2 from abcrown.abcrown_smt import *
3
4 # 1. Define variables exactly as in dReal
5 x = Variable("x")
6 y = Variable("y")
7 z = Variable("z")
8
9 # 2. Formulate constraints using dReal's syntax
  and math functions
10 f_sat = And(
11     0 <= x, x <= 10,
12     0 <= y, y <= 10,
13     0 <= z, z <= 10,
14     sin(x) + cos(y) == z
15 )
16
17 # 3. Check satisfiability with a specified
  delta tolerance
18 result = CheckSatisfiability(f_sat, 0.001)
19
20 print(result)

```

VI. CONTROLLER AND CERTIFICATE SYNTHESIS

In this section, we discuss how to jointly synthesize the controller and the neural certificate through learning (e.g., a learned Lyapunov function or contraction metrics). We note that since formal verification requires the specification to hold for the entire domain, it is much more difficult compared to a normal machine learning task, where certain errors on the test set are tolerable. Therefore, in this setting, a simple random sampling approach to construct the train/test set will not suffice, and we typically design our training algorithms to be verification-aware. One typical training framework is called Counterexample-Guided Inductive Synthesis (CEGIS), which essentially involves finding counterexamples to the verification condition and using them as training data. However, CEGIS exhibits some key disadvantages. For example, training with CEGIS typically requires specially

designed initializations, and the final model obtained may not be verification-friendly [58], [61].

Although there are heuristics that can make CEGIS work better, training a verifier-friendly model purely based on this approach remains a challenge. To conquer this, one prominent direction is certified training, where one directly incorporates the bounds generated by the verifier into the learning process [58], [99]–[102]. Compared to dReal-style solvers, a key practical advantage of α, β -CROWN is that its linear relaxation bounds are **differentiable** with respect to network parameters. At a high level, bound propagation only depends on standard tensor operations (e.g., matrix multiplications), so the resulting output bound is differentiable. This property can be very useful in practice. For example, for a specification of the form $g(x; \theta) > 0$ over an input set \mathcal{B} , α, β -CROWN produces a certified lower bound

$$g(x; \theta) \geq \underline{A}(\theta)x + \underline{b}(\theta), \quad \forall x \in \mathcal{B},$$

and thus a differentiable lower bound on the worst-case violation:

$$\mathcal{L}(\theta) := \underline{g}(\mathcal{B}; \theta) := \inf_{x \in \mathcal{B}} \underline{A}(\theta)x + \underline{b}(\theta). \quad (58)$$

Because $\mathcal{L}(\theta)$ is differentiable, it can be maximized directly using gradient-based optimization to encourage satisfaction of the original specification directly. When this objective is used during training, the procedure is often referred to as **certified training**. Since this training objective is closely related to the verification objective, models trained with this technique can be much verification-friendlier. In the control setting where the domain \mathcal{B} is huge, just as we have discussed about α, β -CROWN, we can also utilize the idea of branch and bound to tighten the bound in training time. Formally, during this training, we maintain a dataset consisting of domains that partition the full domain \mathcal{B} :

$$\mathbb{B} := \{[\underline{x}^{(1)}, \bar{x}^{(1)}], [\underline{x}^{(2)}, \bar{x}^{(2)}], \dots, [\underline{x}^{(n)}, \bar{x}^{(n)}]\}. \quad (59)$$

On each of the subdomains, we use α, β -CROWN to obtain a lower bound $\underline{g}(\underline{x}^{(i)}, \bar{x}^{(i)})$. The loss function can then be defined as

$$L(\theta; \mathbb{B}) = \mathbb{E}_{\mathbb{B}}[\text{ReLU}(-\underline{g}(\underline{x}^{(i)}, \bar{x}^{(i)}))]. \quad (60)$$

Moreover, we can still incorporate the counterexample loss used in the CEGIS framework as an added empirical guard. We shall note that since now the domains are split into smaller pieces, the counterexample finding procedure can also more efficiently find counterexamples and help the learning. When the bound is not tight enough so that the minimization fails to push the lower bound above zero in a particular training subdomain, we further branch it with the heuristics described in section III-D. This branching can further tighten the bounds. We then add the split domains into the training data and remove the original domain.

We note that since this approach directly targets the verification condition and explicitly uses the bound generated by the verifier as a training objective, it can yield models that are much easier to verify. As a comparison, in the 2D

quadrotor environment, the certified training approach can yield a model that is 5 times faster to verify compared to a CEGIS-trained model.

VII. ADVANCED TOPICS

A. Solving Optimization Problems

In this section, we briefly discuss how bound propagation, together with branch and bound, can be used as an efficient nonlinear programming solver. In this case, rather than verifying a specific condition like $F(x) \geq 0$ for all $x \in \mathcal{B}$, our goal is to find the minimizer of F over this box domain, i.e., we wish to solve

$$f^* = \min_{x \in \mathcal{B}} F(x). \quad (61)$$

To efficiently compute this, we shall still continue with the certified lower bound computation with branch-and-bound. We notice that on each of the subdomains \mathcal{B}_i , in addition to the certified lower bounds \underline{F}_i being produced, a PGD run as in the first stage of solving the satisfiability problem could be used to produce feasible upper bounds \overline{F}_i of the problem on each subdomain. Using this upper bound information, it is clear that we can always prune subdomains \mathcal{B}_j with $\underline{F}_j > \min_i \overline{F}_i$, since this subdomain is certified to be above the best solution we have found so far. Now, with continued branch-and-bound, most subdomains will be pruned, leaving the found feasible solution closer to the optimal possible solution. The algorithm will terminate when a computation budget is reached. We note that in this optimization context, when the gap between the best feasible upper bound and the minimum certified lower bound over the remaining subdomains is small, this branch-and-bound procedure also provides an optimality certificate.

B. Other Improvements of Verification

When bounds produced by standard propagation remain loose, the verifier supports several advanced functionalities for further bound tightening. Specifically, α -CROWN [49] tightens bounds by optimizing parameterized local linear relaxations. To resolve persistent looseness from nonlinearities, β -CROWN [51] and GenBaB [55] perform activation branching by partitioning the domains of nonlinear operators and optimizing the resulting Lagrangian dual variables, which can achieve complete verification without relying on input domain branch-and-bound. Furthermore, Clip-and-Verify [56] exploits otherwise discarded affine constraints to continuously prune the input domain and tighten intermediate bounds. Finally, extensions such as GCP-CROWN [52] and BICCOS [54] further strengthen the relaxations by incorporating cutting planes directly into the bound propagation framework.

VIII. CONCLUSIONS

In this tutorial, we presented a unified workflow for certifying learned controllers with the neural network verifier α, β -CROWN. The same framework supports multiple control tasks and usage modes. We also discussed the API of α, β -CROWN, as well as training paradigms such as

CEGIS and certified training for co-synthesizing controllers and verifier-friendly certificates. We hope this tutorial helps bridge control theory and scalable neural network verification, and makes formal certification a more practical component of learning-based control design.

IX. ACKNOWLEDGMENTS

B. Hu is generously supported by the NSF award CAREER-2048168 and the AFOSR award FA9550-23-1-0732. H. Zhang, X. Zhong, and H. Li are supported in part by the AI2050 program at Schmidt Sciences (AI2050 Early Career Fellowship) and NSF (IIS-2331967).

REFERENCES

- [1] E. Kaufmann, L. Bauersfeld, A. Loquercio, M. Müller, V. Koltun, and D. Scaramuzza, “Champion-level drone racing using deep reinforcement learning,” *Nature*, vol. 620, no. 7976, pp. 982–987, 2023.
- [2] X. Zhao, Y. Sun, Y. Li, N. Jia, and J. Xu, “Applications of machine learning in real-time control systems: a review,” *Measurement Science and Technology*, 2024.
- [3] M. Glavic, “(deep) reinforcement learning for electric power system control and related problems: A short review and perspectives,” *Annual Reviews in Control*, vol. 48, pp. 22–35, 2019.
- [4] L. Buşoniu, T. De Bruin, D. Tolić, J. Kober, and I. Palunko, “Reinforcement learning for control: Performance, stability, and deep approximators,” *Annual Reviews in Control*, vol. 46, pp. 8–28, 2018.
- [5] H.-D. Tran, W. Xiang, and T. T. Johnson, “Verification approaches for learning-enabled autonomous cyber–physical systems,” *IEEE Design & Test*, vol. 39, no. 1, pp. 24–34, 2020.
- [6] C. Dawson, S. Gao, and C. Fan, “Safe control with learned certificates: A survey of neural lyapunov, barrier, and contraction methods for robotics and control,” *IEEE Transactions on Robotics*, vol. 39, no. 3, pp. 1749–1767, 2023.
- [7] Y.-C. Chang, N. Roohi, and S. Gao, “Neural lyapunov control,” *Advances in neural information processing systems*, vol. 32, 2019.
- [8] P. Jagtap, S. Soudjani, and M. Zamani, “Formal synthesis of stochastic systems via control barrier certificates,” *IEEE Transactions on Automatic Control*, vol. 66, no. 7, pp. 3097–3110, 2020.
- [9] J. Liu, M. Fitzsimmons, R. Zhou, and Y. Meng, “Formally verified physics-informed neural control lyapunov functions,” in *2025 American Control Conference (ACC)*. IEEE, 2025, pp. 1347–1354.
- [10] J. Liu, Y. Meng, M. Fitzsimmons, and R. Zhou, “Physics-informed neural network lyapunov functions: Pde characterization, learning, and verification,” *Automatica*, vol. 175, p. 112193, 2025.
- [11] Y. Meng, R. Zhou, and J. Liu, “Learning regions of attraction in unknown dynamical systems via zubov-koopman lifting: Regularities and convergence,” *IEEE Transactions on Automatic Control*, 2025.
- [12] J. Liu, Y. Meng, M. Fitzsimmons, and R. Zhou, “Tool lyznet: A lightweight python tool for learning and verifying neural lyapunov functions and regions of attraction,” in *Proceedings of the 27th ACM International Conference on Hybrid Systems: Computation and Control*, 2024, pp. 1–8.
- [13] J. Wang and M. Fazlyab, “Actor-critic physics-informed neural lyapunov control,” *IEEE Control Systems Letters*, 2024.
- [14] A. Edwards, A. Peruffo, and A. Abate, “Fossil 2.0: Formal certificate synthesis for the verification and control of dynamical models,” in *Proceedings of the 27th ACM International Conference on Hybrid Systems: Computation and Control*, 2024, pp. 1–10.
- [15] J. Liu, Y. Meng, M. Fitzsimmons, and R. Zhou, “Towards learning and verifying maximal neural lyapunov functions,” in *2023 62nd IEEE Conference on Decision and Control (CDC)*. IEEE, 2023, pp. 8012–8019.
- [16] S. Gao, S. Kong, and E. M. Clarke, “dreal: An smt solver for nonlinear theories over the reals,” in *International conference on automated deduction*. Springer, 2013, pp. 208–214.
- [17] L. De Moura and N. Björner, “Z3: An efficient smt solver,” in *International conference on Tools and Algorithms for the Construction and Analysis of Systems*. Springer, 2008, pp. 337–340.
- [18] V. Tjeng, K. Xiao, and R. Tedrake, “Evaluating robustness of neural networks with mixed integer programming,” *arXiv preprint arXiv:1711.07356*, 2017.

- [19] G. Katz, C. Barrett, D. L. Dill, K. Julian, and M. J. Kochenderfer, “Reluplex: An efficient smt solver for verifying deep neural networks,” in *International conference on computer aided verification*. Springer, 2017, pp. 97–117.
- [20] G. Katz, D. A. Huang, D. Ibeling, K. Julian, C. Lazarus, R. Lim, P. Shah, S. Thakoor, H. Wu, A. Zeljić *et al.*, “The marabou framework for verification and analysis of deep neural networks,” in *International conference on computer aided verification*. Springer, 2019, pp. 443–452.
- [21] B. Karg and S. Lucia, “Stability and feasibility of neural network-based controllers via output range analysis,” in *2020 59th IEEE Conference on Decision and Control (CDC)*. IEEE, 2020, pp. 4947–4954.
- [22] H. Dai, B. Landry, L. Yang, M. Pavone, and R. Tedrake, “Lyapunov-stable neural-network control,” *arXiv preprint arXiv:2109.14152*, 2021.
- [23] J. Wu, A. Clark, Y. Kantaros, and Y. Vorobeychik, “Neural lyapunov control for discrete-time systems,” *Advances in neural information processing systems*, vol. 36, pp. 2939–2955, 2023.
- [24] A. Papachristodoulou and S. Prajna, “A tutorial on sum of squares techniques for systems analysis,” in *Proceedings of the 2005, American Control Conference, 2005*. IEEE, 2005, pp. 2686–2700.
- [25] H. Yin, P. Seiler, and M. Arcak, “Stability analysis using quadratic constraints for systems with neural network controllers,” *IEEE Transactions on Automatic Control*, vol. 67, no. 4, pp. 1980–1987, 2021.
- [26] H. Dai, C. Jiang, H. Zhang, and A. Clark, “Verification and synthesis of compatible control lyapunov and control barrier functions,” in *2024 IEEE 63rd Conference on Decision and Control (CDC)*. IEEE, 2024, pp. 8178–8185.
- [27] M. Newton and A. Papachristodoulou, “Stability of non-linear neural feedback loops using sum of squares,” in *2022 IEEE 61st Conference on Decision and Control (CDC)*. IEEE, 2022, pp. 6000–6005.
- [28] A. Demailleur, G. Ducard, and C. Onder, “Improved sum-of-squares stability verification of neural-network-based controllers,” *arXiv preprint arXiv:2507.10352*, 2025.
- [29] H. Yin, P. Seiler, M. Jin, and M. Arcak, “Imitation learning with stability and safety guarantees,” *IEEE Control Systems Letters*, vol. 6, pp. 409–414, 2021.
- [30] A. Clark, “A semialgebraic framework for verification and synthesis of control barrier functions,” *IEEE Transactions on Automatic Control*, vol. 70, no. 5, pp. 3101–3116, 2024.
- [31] L. Wei, R. McCloy, and J. Bao, “Control contraction metric synthesis for discrete-time nonlinear systems,” *IFAC-PapersOnLine*, vol. 54, no. 3, pp. 661–666, 2021.
- [32] R. Tedrake, I. R. Manchester, M. Tobenkin, and J. W. Roberts, “Lqr-trees: Feedback motion planning via sums-of-squares verification,” *The International Journal of Robotics Research*, vol. 29, no. 8, pp. 1038–1052, 2010.
- [33] W. Zhao, T. He, T. Wei, S. Liu, and C. Liu, “Safety index synthesis via sum-of-squares programming,” in *American Control Conference*. IEEE, 2023, pp. 732–737.
- [34] H. Hu, Y. Yang, T. Wei, and C. Liu, “Verification of neural control barrier functions with symbolic derivative bounds propagation,” in *Proceedings of The 8th Conference on Robot Learning*, ser. Proceedings of Machine Learning Research, vol. 270. PMLR, 06–09 Nov 2025, pp. 1797–1814.
- [35] H. Zhang, J. Wu, Y. Vorobeychik, and A. Clark, “Exact verification of relu neural control barrier functions,” *Advances in neural information processing systems*, vol. 36, pp. 5685–5705, 2023.
- [36] N. Vertovec, F. B. Mathiesen, T. Badings, L. Laurenti, and A. Abate, “Scalable verification of neural control barrier functions using linear bound propagation,” *arXiv preprint arXiv:2511.06341*, 2025.
- [37] H. Hu, J. Lan, and C. Liu, “Real-time safe control of neural network dynamic models with sound approximation,” in *Learning for Dynamics and Control Conference*, 2024. [Online]. Available: <https://proceedings.mlr.press/v242/hu24a.html>
- [38] J. Li, H. Hu, Y. Yang, and C. Liu, “Verifiable safety q-filters via hamilton-jacobi reachability and multiplicative q-networks,” *IEEE Control Systems Letters*, 2025. [Online]. Available: <https://ieeexplore.ieee.org/stamp/stamp.jsp?tp=&arnumber=11157757>
- [39] E. Wong and Z. Kolter, “Provable defenses against adversarial examples via the convex outer adversarial polytope,” in *International conference on machine learning*. PMLR, 2018, pp. 5286–5295.
- [40] A. Raghunathan, J. Steinhardt, and P. Liang, “Certified defenses against adversarial examples,” *arXiv preprint arXiv:1801.09344*, 2018.
- [41] R. A. Brown, E. Schmerling, N. Azizan, and M. Pavone, “A unified view of sdp-based neural network verification through completely positive programming,” in *International conference on artificial intelligence and statistics*. PMLR, 2022, pp. 9334–9355.
- [42] T. Gehr, M. Mirman, D. Drachler-Cohen, P. Tsankov, S. Chaudhuri, and M. Vechev, “Ai2: Safety and robustness certification of neural networks with abstract interpretation,” in *2018 IEEE symposium on security and privacy (SP)*. IEEE, 2018, pp. 3–18.
- [43] G. Singh, T. Gehr, M. Mirman, M. Püschel, and M. Vechev, “Fast and effective robustness certification,” *Advances in neural information processing systems*, vol. 31, 2018.
- [44] H. Zhang, T.-W. Weng, P.-Y. Chen, C.-J. Hsieh, and L. Daniel, “Efficient neural network robustness certification with general activation functions,” *Advances in Neural Information Processing Systems*, vol. 31, pp. 4939–4948, 2018. [Online]. Available: <https://arxiv.org/pdf/1811.00866.pdf>
- [45] S. Jafarpour, A. Harapanahalli, and S. Coogan, “Efficient interaction-aware interval analysis of neural network feedback loops,” *IEEE Transactions on Automatic Control*, vol. 69, no. 12, pp. 8706–8721, 2024.
- [46] —, “Interval reachability of nonlinear dynamical systems with neural network controllers,” in *Learning for Dynamics and Control Conference*. PMLR, 2023, pp. 12–25.
- [47] S. Goyal, K. Dvijotham, R. Stanforth, R. Bunel, C. Qin, J. Uesato, R. Arandjelovic, T. Mann, and P. Kohli, “On the effectiveness of interval bound propagation for training verifiably robust models,” *arXiv preprint arXiv:1810.12715*, 2018.
- [48] H. Salman, G. Yang, H. Zhang, C.-J. Hsieh, and P. Zhang, “A convex relaxation barrier to tight robustness verification of neural networks,” *Advances in Neural Information Processing Systems*, vol. 32, pp. 9835–9846, 2019.
- [49] K. Xu, Z. Shi, H. Zhang, Y. Wang, K.-W. Chang, M. Huang, B. Kailkhura, X. Lin, and C.-J. Hsieh, “Automatic perturbation analysis for scalable certified robustness and beyond,” *Advances in Neural Information Processing Systems*, vol. 33, 2020.
- [50] K. Xu, H. Zhang, S. Wang, Y. Wang, S. Jana, X. Lin, and C.-J. Hsieh, “Fast and Complete: Enabling complete neural network verification with rapid and massively parallel incomplete verifiers,” in *International Conference on Learning Representations*, 2021. [Online]. Available: <https://openreview.net/forum?id=nVZtXBI6LNn>
- [51] S. Wang, H. Zhang, K. Xu, X. Lin, S. Jana, C.-J. Hsieh, and J. Z. Kolter, “Beta-CROWN: Efficient bound propagation with per-neuron split constraints for complete and incomplete neural network verification,” *Advances in Neural Information Processing Systems*, vol. 34, 2021.
- [52] H. Zhang, S. Wang, K. Xu, L. Li, B. Li, S. Jana, C.-J. Hsieh, and J. Z. Kolter, “General cutting planes for bound-propagation-based neural network verification,” *Advances in Neural Information Processing Systems*, 2022.
- [53] S. Kotha, C. Brix, J. Z. Kolter, K. Dvijotham, and H. Zhang, “Provably bounding neural network preimages,” in *Advances in Neural Information Processing Systems*, A. Oh, T. Neumann, A. Globerson, K. Saenko, M. Hardt, and S. Levine, Eds., vol. 36. Curran Associates, Inc., 2023, pp. 80 270–80 290.
- [54] D. Zhou, C. Brix, G. A. Hanasusanto, and H. Zhang, “Scalable neural network verification with branch-and-bound inferred cutting planes,” in *The Thirty-eighth Annual Conference on Neural Information Processing Systems*, 2024.
- [55] Z. Shi, Q. Jin, Z. Kolter, S. Jana, C.-J. Hsieh, and H. Zhang, “Neural network verification with branch-and-bound for general nonlinearities,” in *International Conference on Tools and Algorithms for the Construction and Analysis of Systems*, 2025.
- [56] D. Zhou, J. Chavez, H. Chen, G. A. Hanasusanto, and H. Zhang, “Clip-and-verify: Linear constraint-driven domain clipping for accelerating neural network verification,” *arXiv preprint arXiv:2512.11087*, 2025.
- [57] L. Yang, H. Dai, Z. Shi, C.-J. Hsieh, R. Tedrake, and H. Zhang, “Lyapunov-stable neural control for state and output feedback: A novel formulation,” *arXiv preprint arXiv:2404.07956*, 2024.
- [58] Z. Shi, H. Li, C.-J. Hsieh, and H. Zhang, “Certified training with branch-and-bound for lyapunov-stable neural control,” *arXiv preprint arXiv:2411.18235*, 2024.

- [59] H. Li, X. Zhong, B. Hu, and H. Zhang, "Neural contraction metrics with formal guarantees for discrete-time nonlinear dynamical systems," *arXiv preprint arXiv:2504.17102*, 2025.
- [60] M. Serry, H. Li, R. Zhou, H. Zhang, and J. Liu, "Safe domains of attraction for discrete-time nonlinear systems: Characterization and verifiable neural network estimation," *arXiv preprint arXiv:2506.13961*, 2025.
- [61] H. Li, X. Zhong, B. Hu, and H. Zhang, "Two-stage learning of stabilizing neural controllers via zubov sampling and iterative domain expansion," *arXiv preprint arXiv:2506.01356*, 2025.
- [62] X. Chen, E. Ábrahám, and S. Sankaranarayanan, "Flow*: An analyzer for non-linear hybrid systems," in *International Conference on Computer Aided Verification*. Springer, 2013, pp. 258–263.
- [63] M. Althoff, G. Frehse, and A. Girard, "Set propagation techniques for reachability analysis," *Annual Review of Control, Robotics, and Autonomous Systems*, vol. 4, no. 1, pp. 369–395, 2021.
- [64] H.-D. Tran, X. Yang, D. Manzananas Lopez, P. Musau, L. V. Nguyen, W. Xiang, S. Bak, and T. T. Johnson, "Nnv: the neural network verification tool for deep neural networks and learning-enabled cyber-physical systems," in *International conference on computer aided verification*. Springer, 2020, pp. 3–17.
- [65] C. Zhang, W. Ruan, and P. Xu, "Reachability analysis of neural network control systems," in *Proceedings of the AAAI Conference on Artificial Intelligence*, vol. 37, no. 12, 2023, pp. 15 287–15 295.
- [66] Y. Zhang, H. Zhang, and X. Xu, "Reachability analysis of neural network control systems with tunable accuracy and efficiency," *IEEE Control Systems Letters*, vol. 8, pp. 1697–1702, 2024.
- [67] A. Abate, S. Bogomolov, A. Edwards, K. Potomkin, S. Soudjani, and P. Zuliani, "Safe reach set computation via neural barrier certificates," *IFAC-PapersOnLine*, vol. 58, no. 11, pp. 107–114, 2024.
- [68] K. Shen and G. Chou, "Parallel differentiable reachability for learning and planning with certified neural dynamics and controllers," in *Proceedings of Robotics: Science and Systems (RSS)*, 2026.
- [69] S. Coogan and M. Arcak, "Efficient finite abstraction of mixed monotone systems," in *Proceedings of the 18th International Conference on Hybrid Systems: Computation and Control*, 2015, pp. 58–67.
- [70] —, "Finite abstraction of mixed monotone systems with discrete and continuous inputs," *Nonlinear Analysis: Hybrid Systems*, vol. 23, pp. 254–271, 2017.
- [71] S. Coogan, "Mixed monotonicity for reachability and safety in dynamical systems," in *2020 59th IEEE Conference on Decision and Control (CDC)*. IEEE, 2020, pp. 5074–5085.
- [72] M. Dutreix and S. Coogan, "Specification-guided verification and abstraction refinement of mixed monotone stochastic systems," *IEEE Transactions on Automatic Control*, vol. 66, no. 7, pp. 2975–2990, 2020.
- [73] C. Sidrane, A. Maleki, A. Irfan, and M. J. Kochenderfer, "Overt: An algorithm for safety verification of neural network control policies for nonlinear systems," *Journal of Machine Learning Research*, vol. 23, no. 117, pp. 1–45, 2022.
- [74] Y. Meng, R. Zhou, and J. Liu, "Zubov-koopman learning of maximal lyapunov functions," in *2024 American Control Conference (ACC)*. IEEE, 2024, pp. 4020–4025.
- [75] Y. Meng and J. Liu, "Towards learning and verifying maximal lyapunov-barrier functions with a zubov pde formulation," *arXiv preprint arXiv:2511.09523*, 2025.
- [76] J. Liu, "Formal verification of control lyapunov-barrier functions for safe stabilization with bounded controls," *arXiv preprint arXiv:2511.10510*, 2025.
- [77] A. D. Ames, X. Xu, J. W. Grizzle, and P. Tabuada, "Control barrier function based quadratic programs for safety critical systems," *IEEE Transactions on Automatic Control*, vol. 62, no. 8, pp. 3861–3876, 2016.
- [78] A. Robey, H. Hu, L. Lindemann, H. Zhang, D. V. Dimarogonas, S. Tu, and N. Matni, "Learning control barrier functions from expert demonstrations," in *2020 59th IEEE Conference on Decision and Control (CDC)*. Ieee, 2020, pp. 3717–3724.
- [79] H. Dai and F. Permenter, "Convex synthesis and verification of control-lyapunov and barrier functions with input constraints," in *2023 American Control Conference (ACC)*. IEEE, 2023, pp. 4116–4123.
- [80] C. Dawson, Z. Qin, S. Gao, and C. Fan, "Safe nonlinear control using robust neural lyapunov-barrier functions," in *Conference on Robot Learning*. PMLR, 2022, pp. 1724–1735.
- [81] H. Tsukamoto and S.-J. Chung, "Neural contraction metrics for robust estimation and control: A convex optimization approach," *IEEE Control Systems Letters*, vol. 5, no. 1, pp. 211–216, 2020.
- [82] H. Tsukamoto, S.-J. Chung, and J.-J. E. Slotine, "Neural stochastic contraction metrics for learning-based control and estimation," *IEEE Control Systems Letters*, vol. 5, no. 5, pp. 1825–1830, 2020.
- [83] H. Tsukamoto, S.-J. Chung, J.-J. Slotine, and C. Fan, "A theoretical overview of neural contraction metrics for learning-based control with guaranteed stability," in *2021 60th IEEE Conference on Decision and Control (CDC)*. IEEE, 2021, pp. 2949–2954.
- [84] D. Sun, S. Jha, and C. Fan, "Learning certified control using contraction metric," in *Conference on Robot Learning*. PMLR, 2021, pp. 1519–1539.
- [85] K. Shen, J. Yu, J. Barreiros, H. Zhang, and Y. Li, "Bab-nd: Long-horizon motion planning with branch-and-bound and neural dynamics," *arXiv preprint arXiv:2412.09584*, 2024.
- [86] A. Abate, C. David, P. Kesseli, D. Kroening, and E. Polgreen, "Counterexample guided inductive synthesis modulo theories," in *International Conference on Computer Aided Verification*. Springer, 2018, pp. 270–288.
- [87] H. Ravanbakhsh and S. Sankaranarayanan, "Counterexample guided synthesis of switched controllers for reach-while-stay properties," *arXiv preprint arXiv:1505.01180*, 2015.
- [88] A. Abate, D. Ahmed, M. Giacobbe, and A. Peruffo, "Formal synthesis of lyapunov neural networks," *IEEE Control Systems Letters*, vol. 5, no. 3, pp. 773–778, 2020.
- [89] D. Masti, F. Fabiani, G. Gnecco, and A. Bemporad, "Counterexample guided inductive synthesis of control lyapunov functions for uncertain systems," *IEEE Control Systems Letters*, vol. 7, pp. 2047–2052, 2023.
- [90] H. Dai, B. Landry, M. Pavone, and R. Tedrake, "Counter-example guided synthesis of neural network lyapunov functions for piecewise linear systems," in *2020 59th IEEE Conference on Decision and Control (CDC)*. IEEE, 2020, pp. 1274–1281.
- [91] H. Ravanbakhsh and S. Sankaranarayanan, "Robust controller synthesis of switched systems using counterexample guided framework," in *Proceedings of the 13th International Conference on Embedded Software*, 2016, pp. 1–10.
- [92] M. Mirman, T. Gehr, and M. Vechev, "Differentiable abstract interpretation for provably robust neural networks," in *International Conference on Machine Learning*. PMLR, 2018, pp. 3578–3586.
- [93] H. K. Khalil and J. W. Grizzle, *Nonlinear systems*. Prentice hall Upper Saddle River, NJ, 2002, vol. 3.
- [94] A. M. Lyapunov, "The general problem of the stability of motion," *International journal of control*, vol. 55, no. 3, pp. 531–534, 1992.
- [95] R. R. Bunel, I. Turkaslan, P. Torr, P. Kohli, and P. K. Mudigonda, "A unified view of piecewise linear neural network verification," *Advances in neural information processing systems*, vol. 31, 2018.
- [96] A. Madry, A. Makelov, L. Schmidt, D. Tsipras, and A. Vladu, "Towards deep learning models resistant to adversarial attacks," *arXiv preprint arXiv:1706.06083*, 2017.
- [97] N. Bof, R. Carli, and L. Schenato, "Lyapunov theory for discrete time systems," *arXiv preprint arXiv:1809.05289*, 2018.
- [98] D. N. Tran, B. S. Rüffer, and C. M. Kellett, "Convergence properties for discrete-time nonlinear systems," *IEEE Transactions on Automatic Control*, vol. 64, no. 8, pp. 3415–3422, 2018.
- [99] H. Zhang, H. Chen, C. Xiao, S. Goyal, R. Stanford, B. Li, D. Boning, and C.-J. Hsieh, "Towards stable and efficient training of verifiably robust neural networks," *arXiv preprint arXiv:1906.06316*, 2019.
- [100] Z. Shi, Y. Wang, H. Zhang, J. Yi, and C.-J. Hsieh, "Fast certified robust training with short warmup," *Advances in Neural Information Processing Systems*, vol. 34, pp. 18 335–18 349, 2021.
- [101] S. Lee, W. Lee, J. Park, and J. Lee, "Towards better understanding of training certifiably robust models against adversarial examples," *Advances in Neural Information Processing Systems*, vol. 34, pp. 953–964, 2021.
- [102] Y. Mao, M. N. Müller, M. Fischer, and M. Vechev, "Understanding certified training with interval bound propagation," *arXiv preprint arXiv:2306.10426*, 2023.